Extended X-Ray Absorption Fine Structure

Lecture series:
Modern Methods in Heterogeneous Catalysis Research

Berlin, Dec 4th 2009

Malte Behrens, FHI-AC
behrens@fhi-berlin.mpg.de

Outline

- Basics
  - Fundamentals
  - What can we learn from an EXAFS experiment?

- How to perform an EXAFS experiment?
  - Synchroton radiation
  - Experimental setup, detection

- How extract information from am EXAFS spectrum
  - The EXAFS equation
  - data treatment

- Examples
 - Application in heterogeneous catalysis

History

- *1895*   Röntgen discovered X-rays

- *1913*   Maurice de Broglie measured first absorption edge

- *1920*   Fricke observed fine structure above X-ray absorption edges

- *1930*   Kronig proposed a LRO theory based on crystal periodicity; then a SRO theory to explain EXAFS in $GeCl_4$ molecule

- *1960*   Van Nordstrand improved XAS instrumentation

  Used fingerprint ID and valence shift to characterize catalysts

- *1970*   Sayers, Stern, and Lytle: Modern theory, FT of EXAFS

- *1974*   Synchrotron X-radiation available at Stanford, CA

- *1994*   Opening of ESRF (Grenoble); 3rd Generation Synchrotron Sources

Acronyms

- XAS **X**-ray **A**bsorption **S**pectroscopy

- XAFS **X**-ray **A**bsorption **F**ine **S**tructure

- EXAFS **E**xtended **X**-ray **A**bsorption **F**ine **S**tructure

- XANES **X**-ray **A**bsorption **N**ear **E**dge **S**tructure

- NEXAFS **N**ear **E**dge **X**-ray **A**bsorption **F**ine **S**tructure

Principle
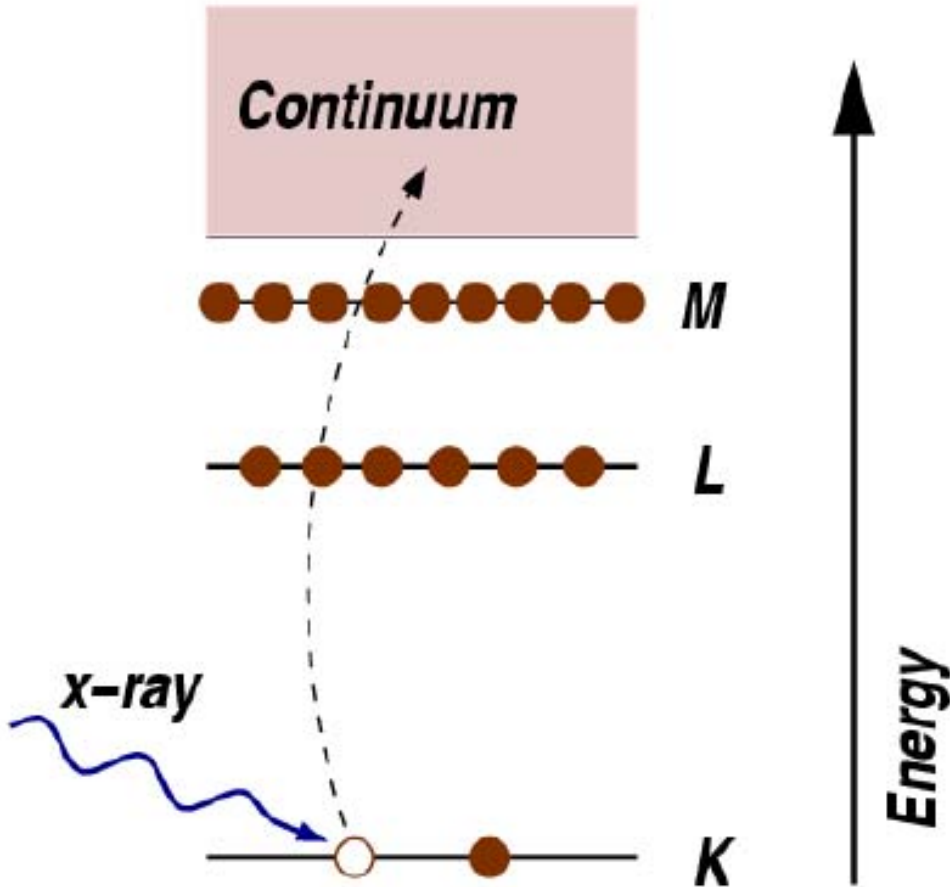
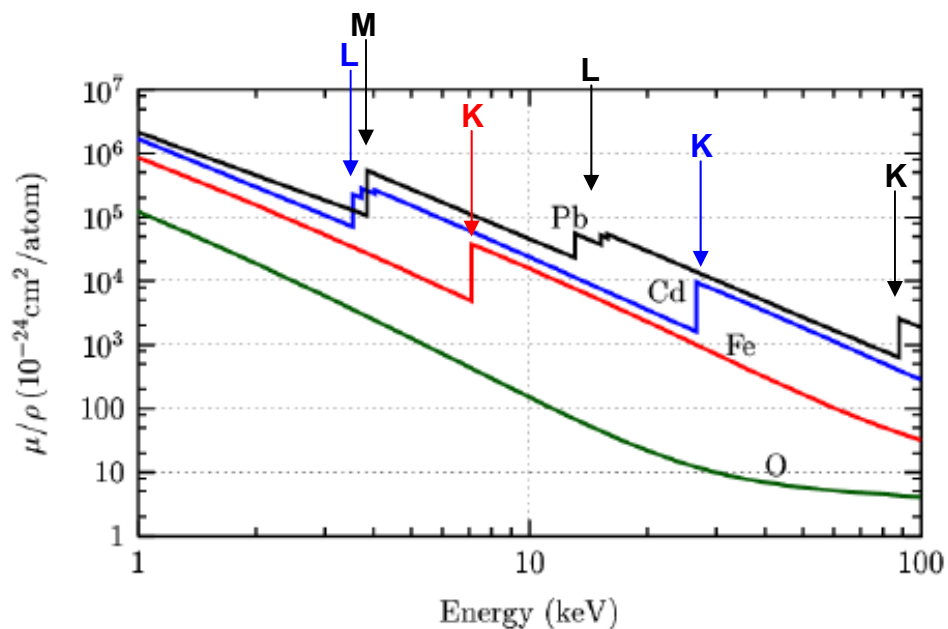- X-ray photons from the incoming beam eject core electron beyond the ionization threshold
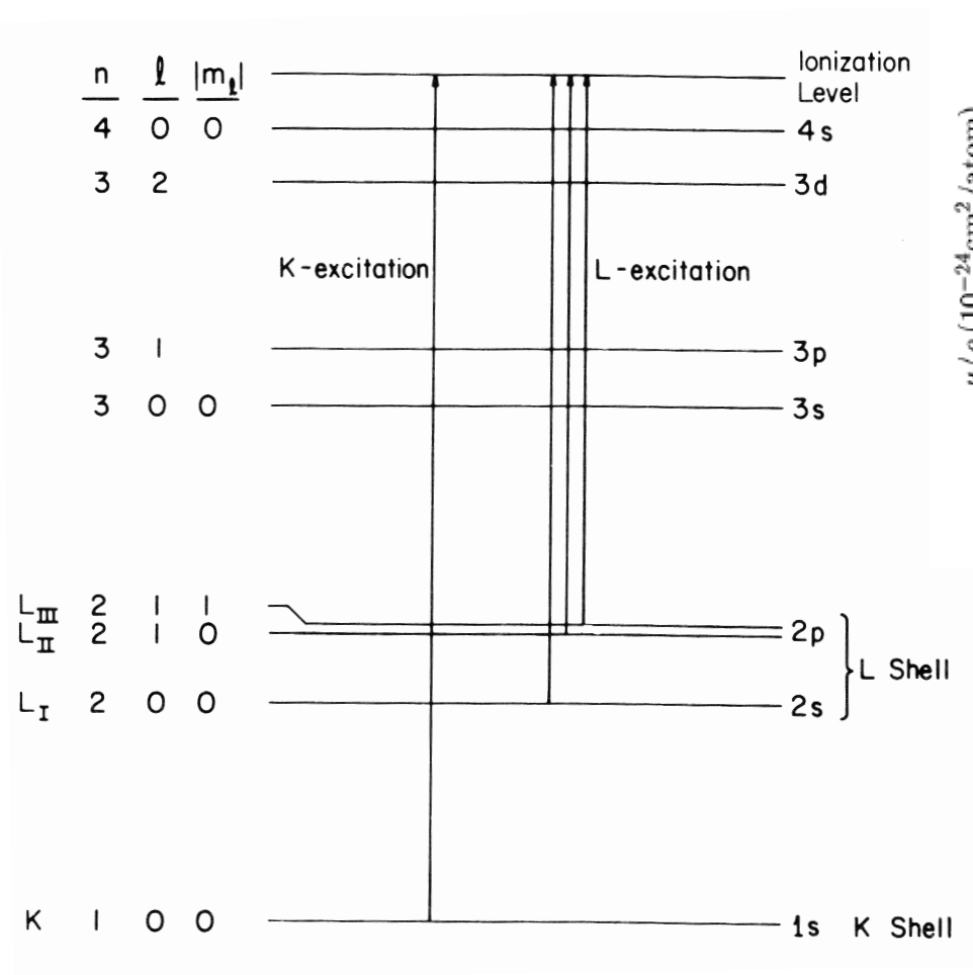
- The atom is in an excited state, i.e. there is a core hole. Electron ejected is called a photo-electron

- The x-ray intensity is measured before and after the sample and the X-ray absorption coefficient μ is calculated

$$I = I_0 e^{-\mu t}$$
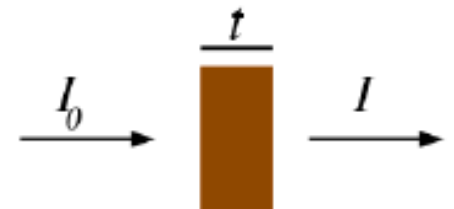
X-ray photon absorption

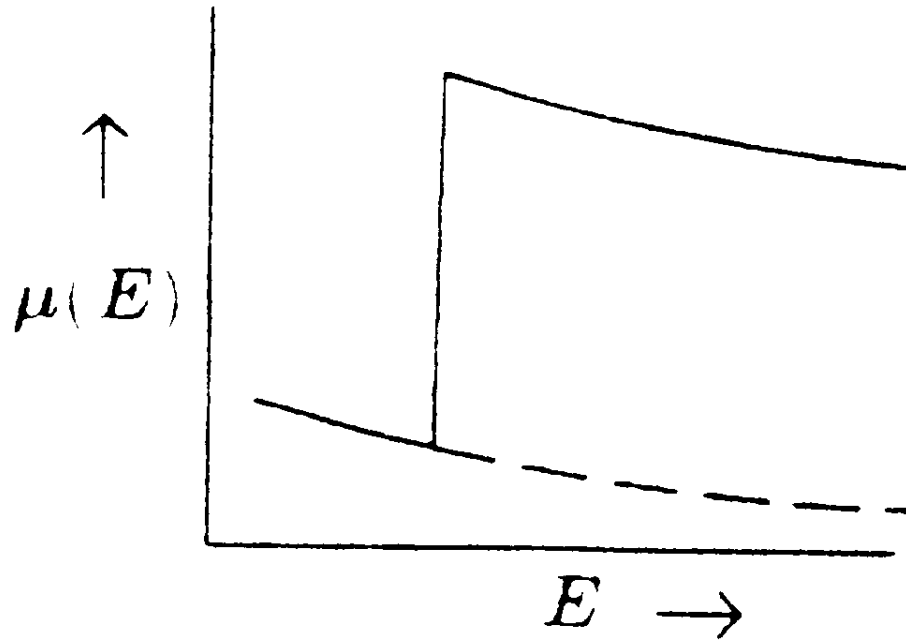sharp absorption edges in μ

↓

characteristic core level energies

EXAFS is elementally specific

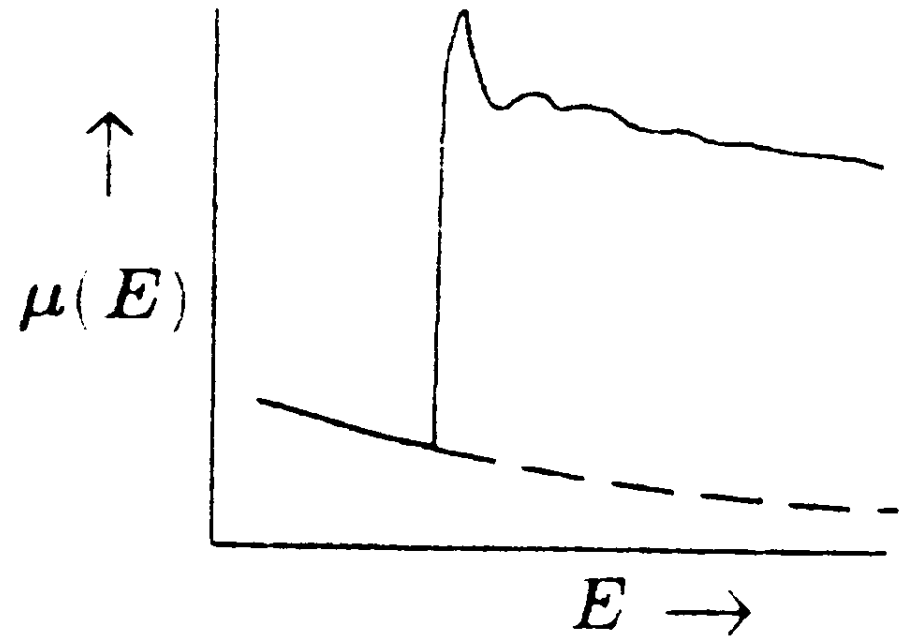L.H. Schwarz, J.B. Cohen / M. Newville
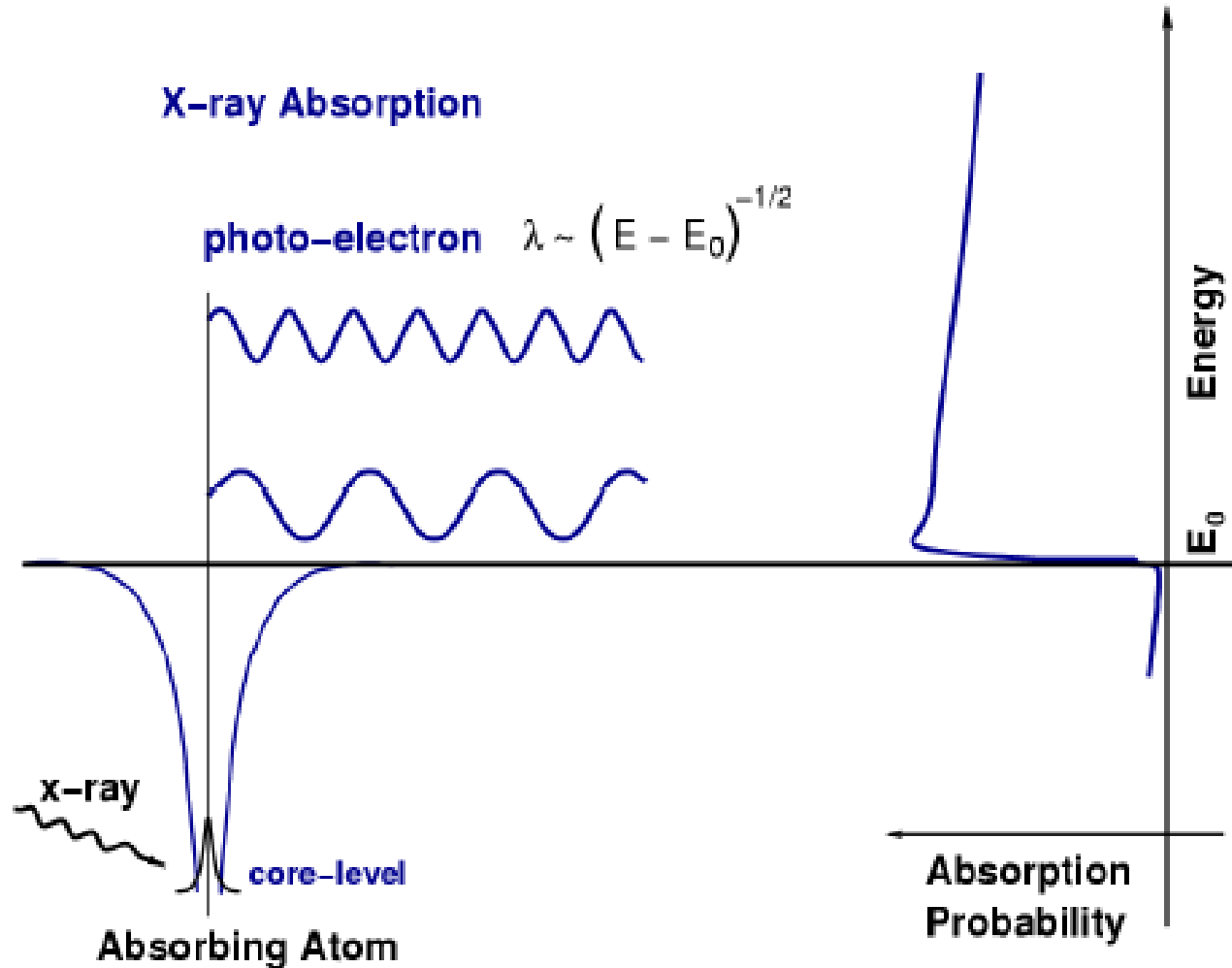
Elements for EXAFS

T. Ressler

Fine structure

Isolated atom

Atom with neighbors

EXAFS contains information about the local environment of the absorber

Isolated atom
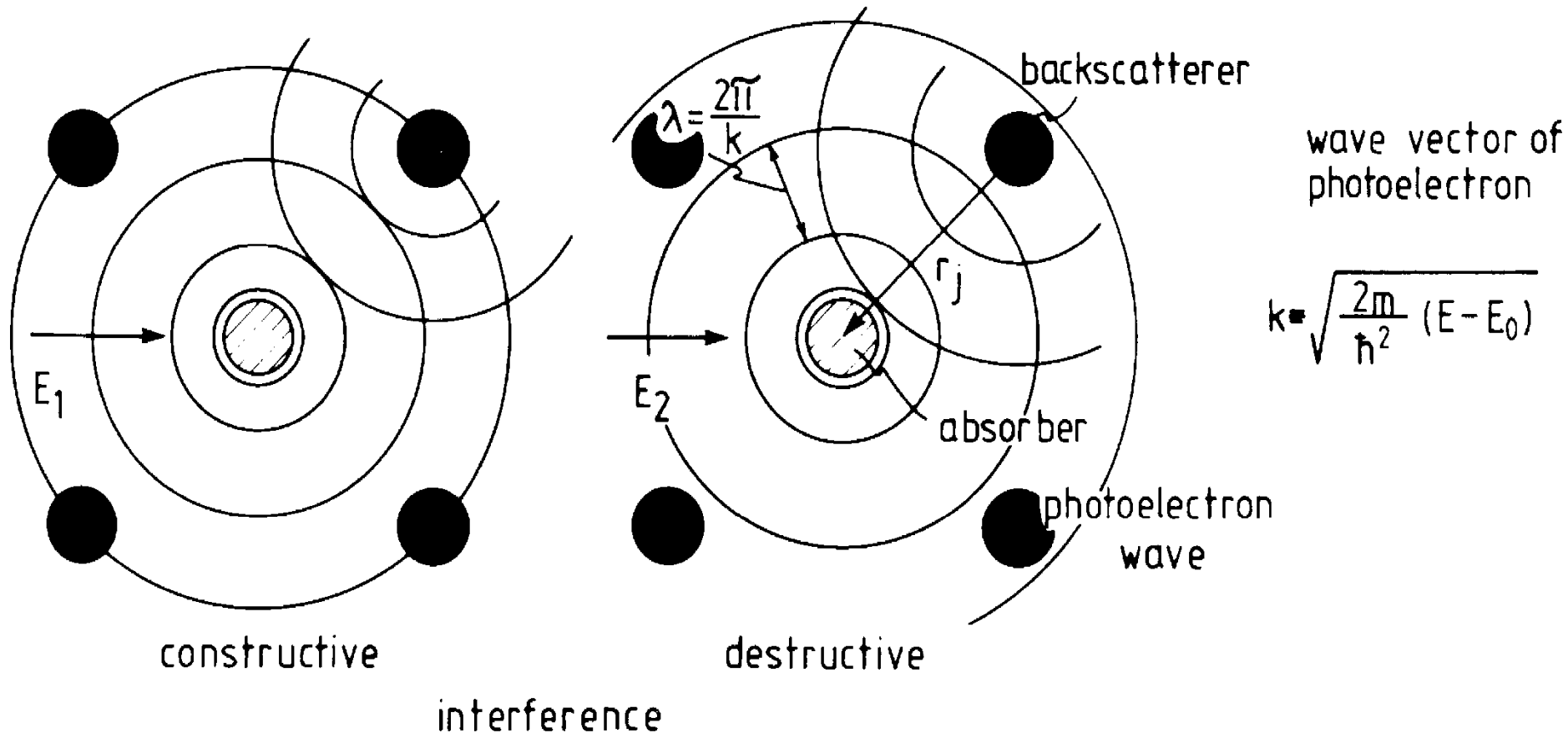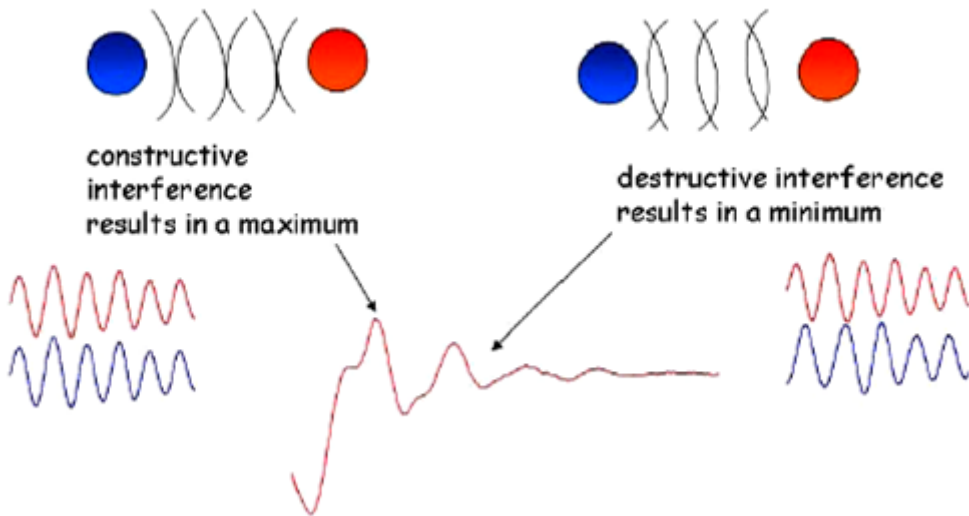

X-ray Absorption

photo-electron $\lambda \sim \left(E - E_0 \right)^{-1/2}$

x-ray

core-level

Absorbing Atom

Energy

E_0

Absorption
Probability

M. Newville

The origin of fine structure

X-ray Absorption Fine-Structure

photo-electron $\lambda \sim \left(E - E_0 \right)^{-1/2}$

Energy

XAFS

XANES

E_0

x-ray

core-level

Absorption Probability

Absorbing Atom   Scattering Atom

Interference effects

constructive

interference

destructive

$$\lambda = \frac{2\pi}{k}$$

backscatterer

r_j

absorber

photoelectron wave

wave vector of photoelectron

$$k = \sqrt{\frac{2m}{\hbar^2}(E - E_0)}$$
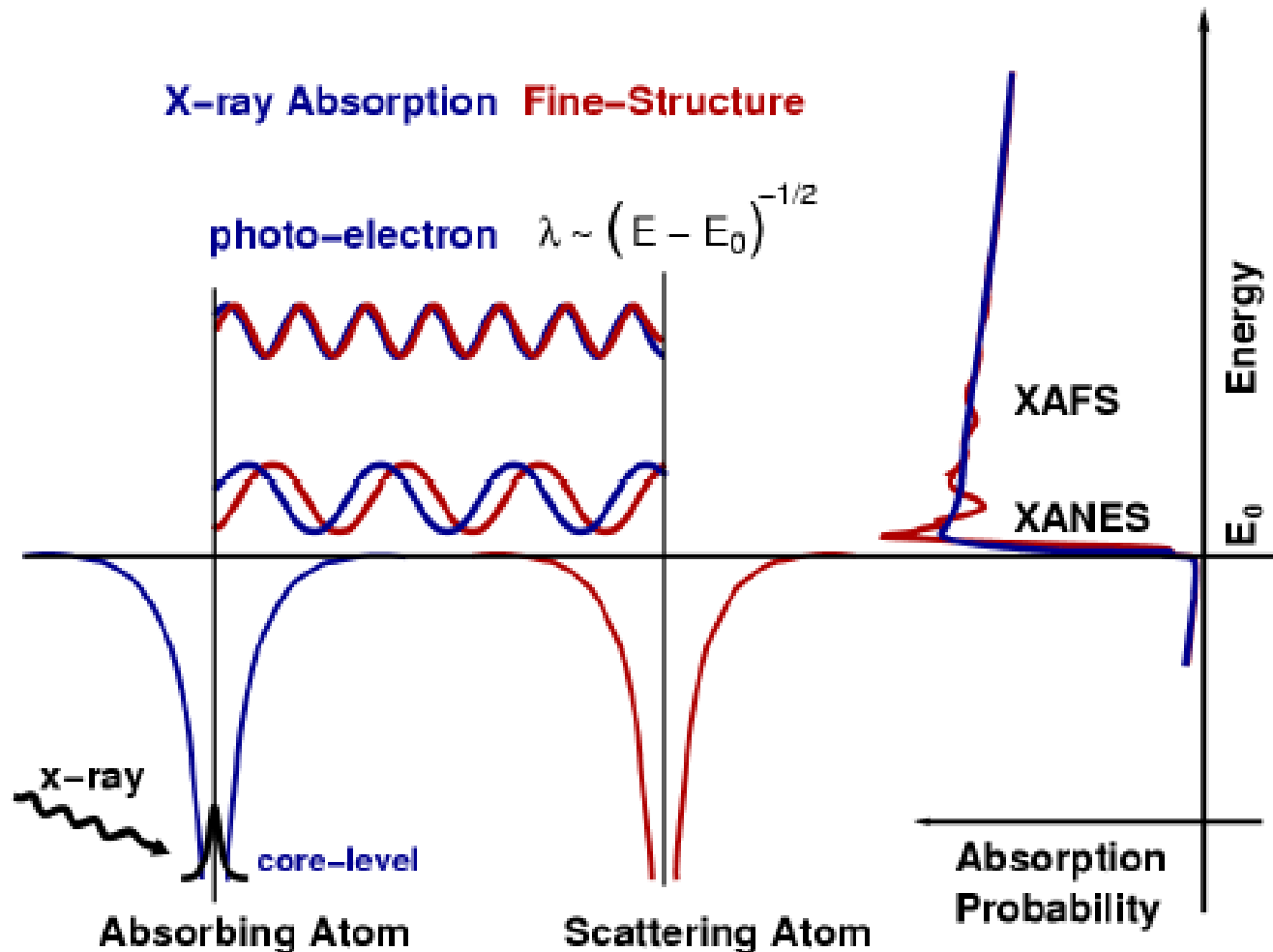
EXAFS: Interference phenomenon between outgoing photo-electron wave and backscattered wave

EXAFS oscillations

constructive interference results in a maximum

destructive interference results in a minimum

Information about interatomic distances

Information about coordination numbers

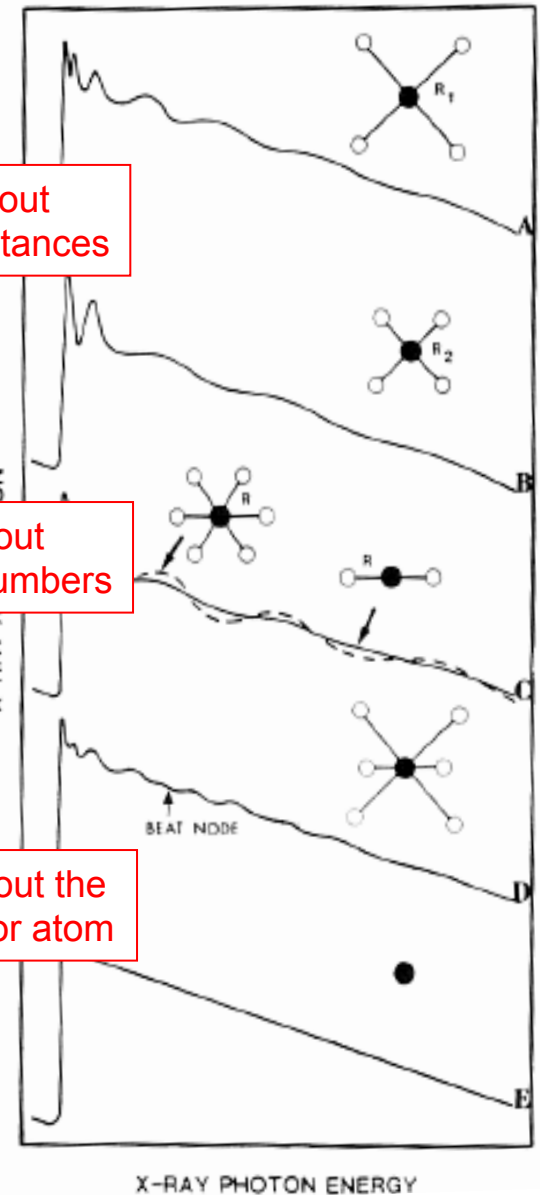Information about the type of neighbor atom

EXAFS spectrum comprised of a series of sine waves of different amplitude representative of the different scattering paths undertaken by the photoelectron wave.
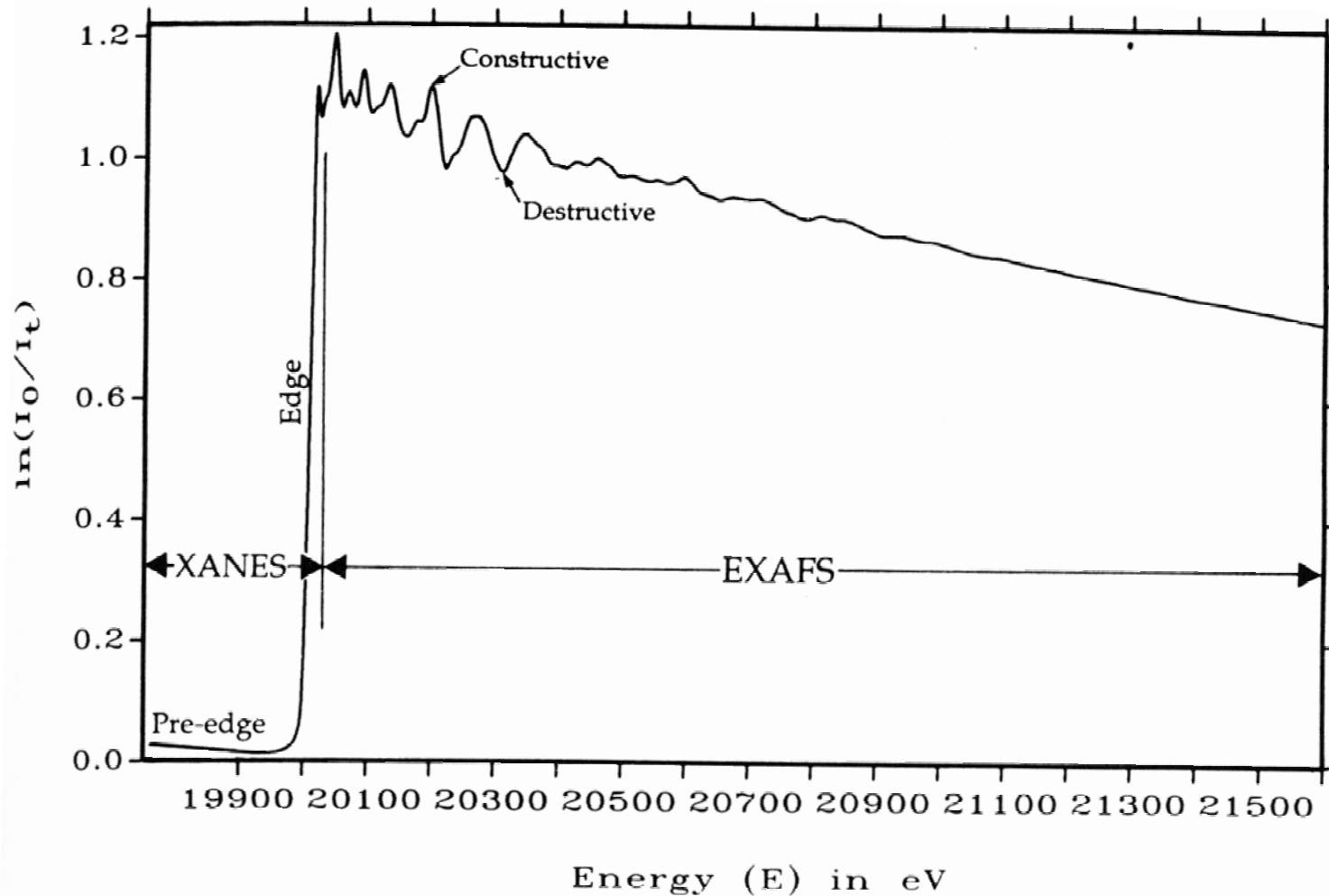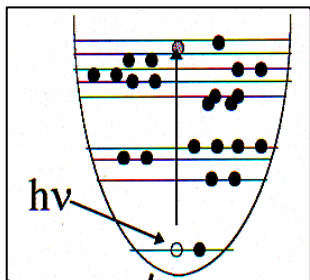
X-RAY ABSORPTION

R_1

R_2

R

BEAT NODE

X-RAY PHOTON ENERGY

A

B

C

D

E

S. Bare

M.R. Antonio

XAFS spectrum (Mo-K)

XANES region

Pre-edge + edge + ca. 50 eV above edge

Dipole transition ($\Delta l = \pm 1$)

s – p
  K edge [1s - 3p]
  L_I edge [2s - 5p]

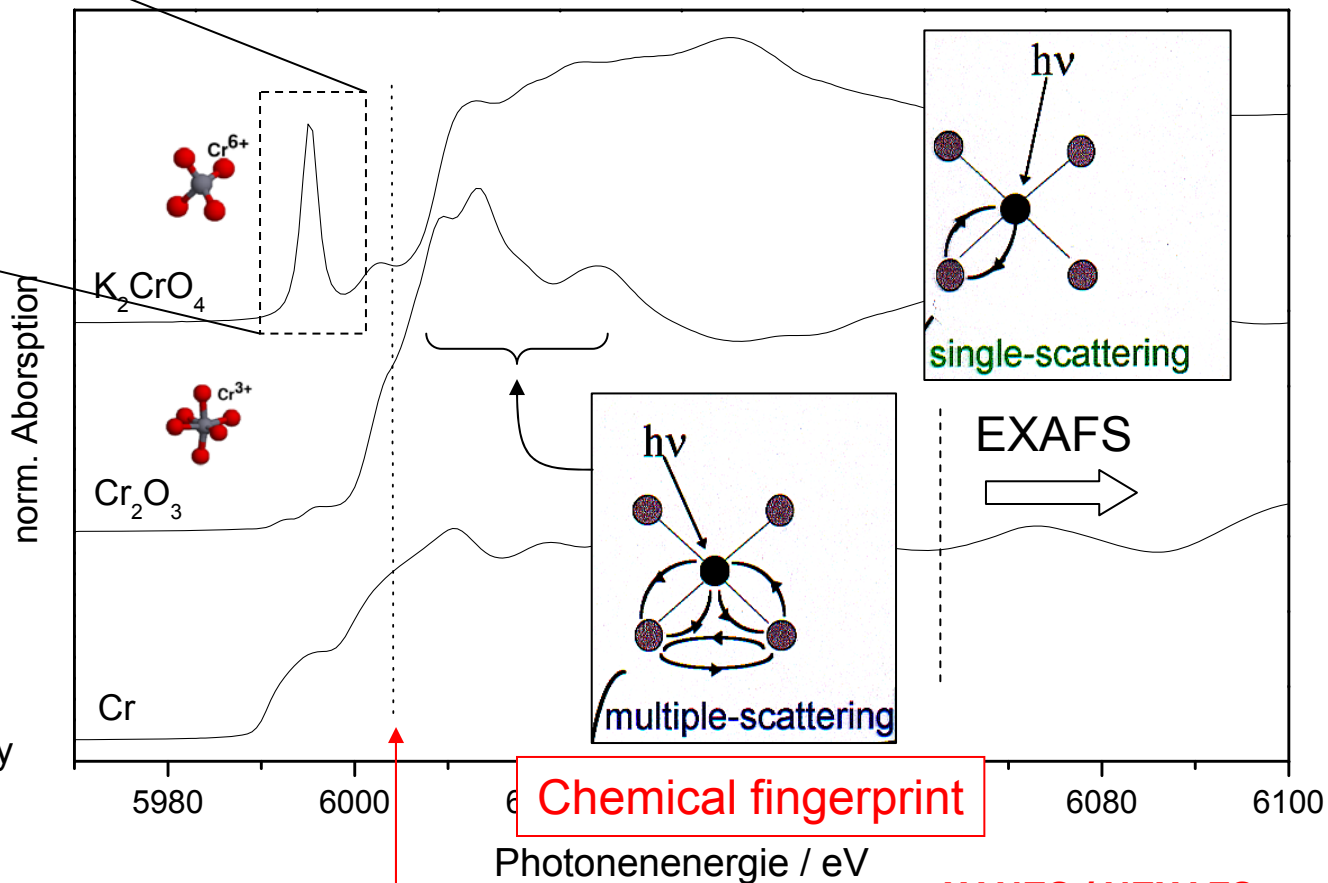p – d
  L_{II} edge [$2p_{1/2}$ - $5d_{3/2}$]
  L_{III} edge [$2p_{3/2}$ - $5d_{5/2}$]

s→ d is dipole forbidden for regular octaherale site symmetry

becomes partially allowed upon distortion and elemination of the center of inversion (p-d hydbridization - open d shell)

T. Ressler

norm. Aborsption

Photonenenergie / eV

5980   6000   6   6080   6100

K_2CrO_4

Cr^{6+}

Cr_2O_3

Cr^{3+}

Cr

single-scattering

multiple-scattering

EXAFS

Chemical fingerprint

Information about oxidation state

XANES / NEXAFS:
Lectures by
A. Knop-Gericke,
K. Hermann

# What do we learn from EXAFS?

- EXAFS gives information about the local environment (up to ca. 6 Å) around a specific type of absorber atom
  - Distance to neighboring atoms
  - Type of neighboring atoms
  - Number of neighboring atoms

- XANES gives information about the
  - oxidation state of the absorber
  - local geometry around the absorber

EXAFS is

- independent of long range order
  - complementary to diffraction
  - gases, liquids, amorphous and crystalline solids
  - highly dispersed phases (catalysis!)

- in general a bulk technique, but has a detection limit in the ppm range
  - Nanoparticles, diluted systems, promoters (catalysis!)

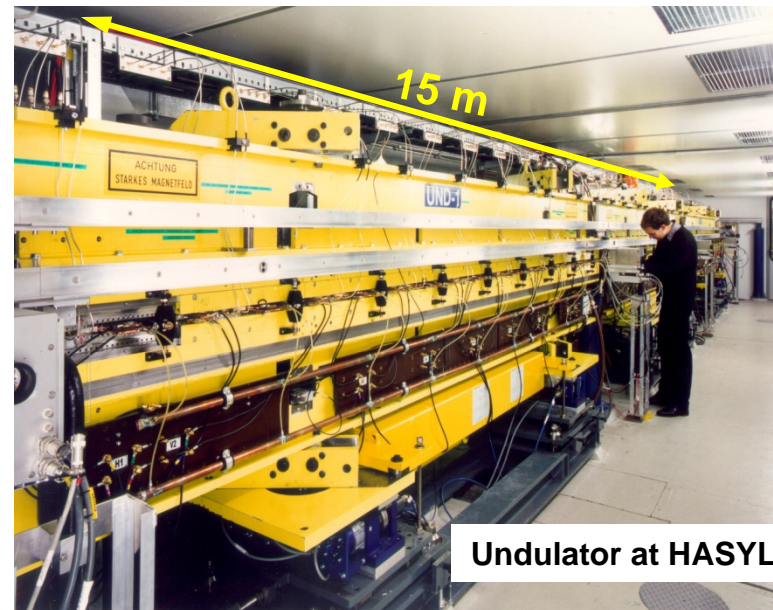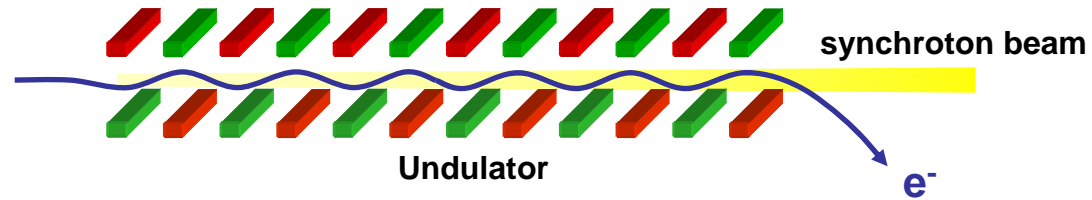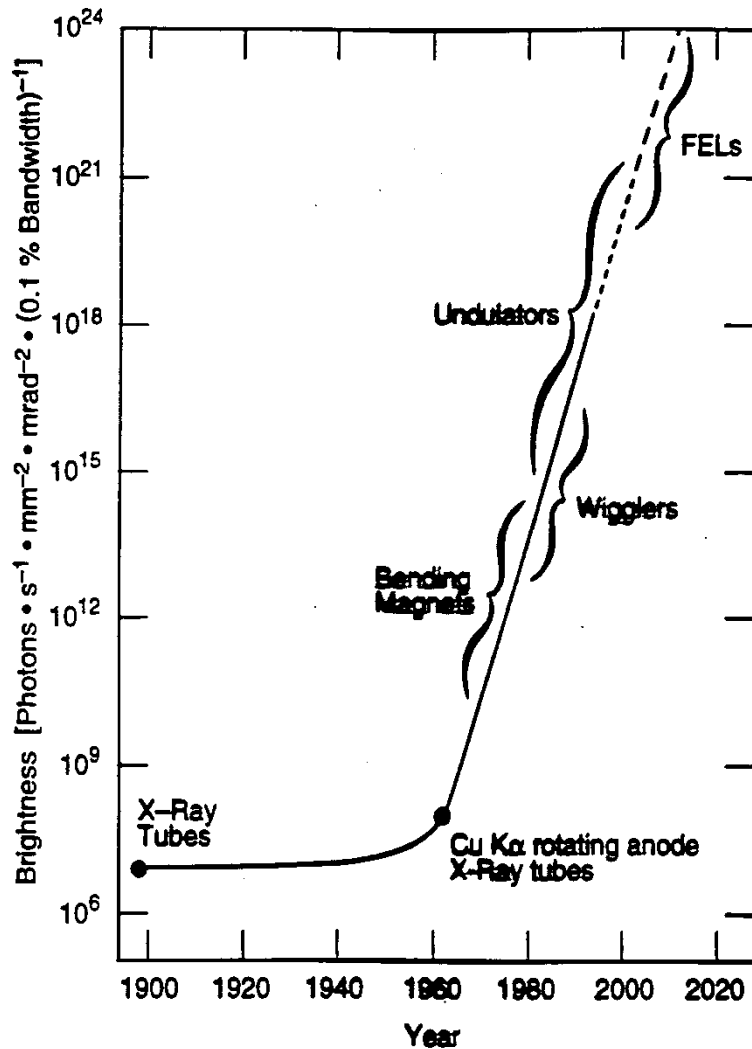- applicable in-situ (catalysis!)

EXAFS (in-situ) experiment

S. Bare
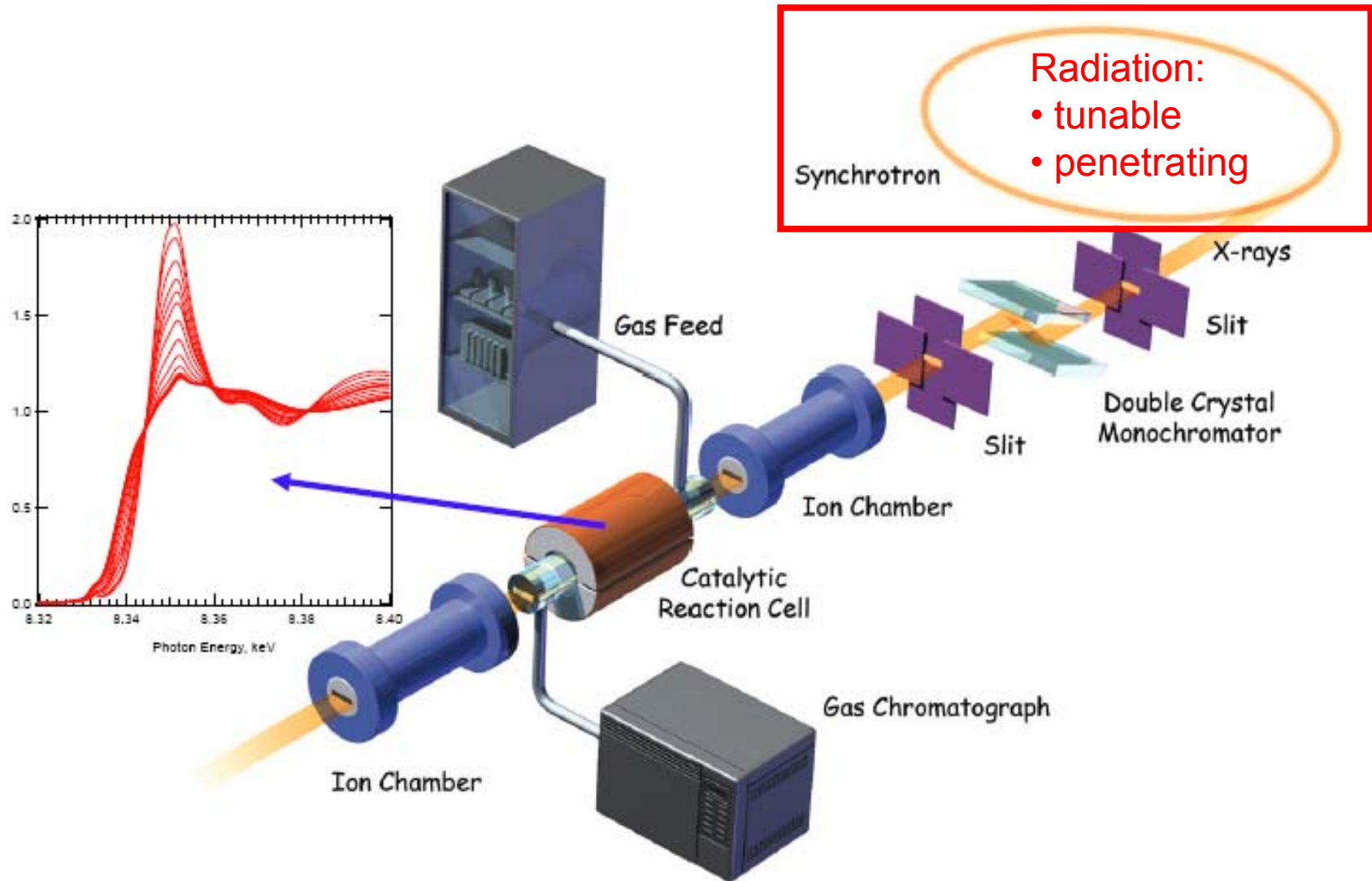
X-ray source: Synchroton

- Electrons near relativistic energies are confined to a circular orbit
- They give off energy as they are deflected
- Synchroton radiation
  - tunable: IR (0.1 mm) to hard X-rays (0.01 nm)
  - high intensity: 10^6 x higher than lab X-ray tubes
  - high collimation
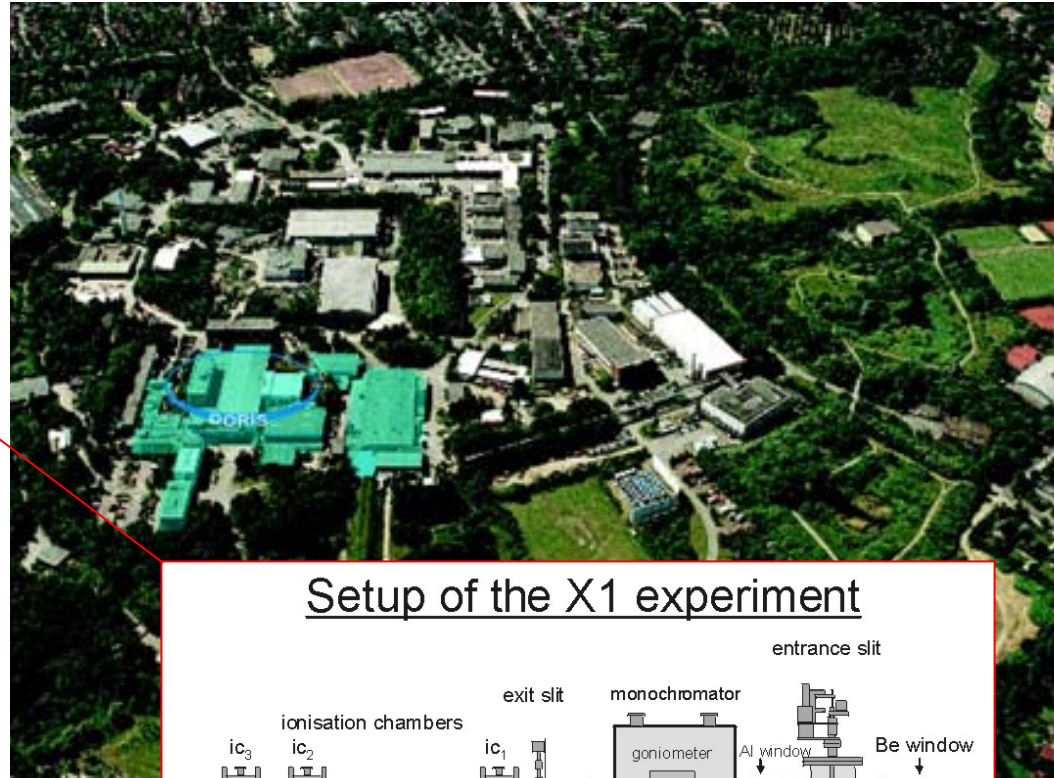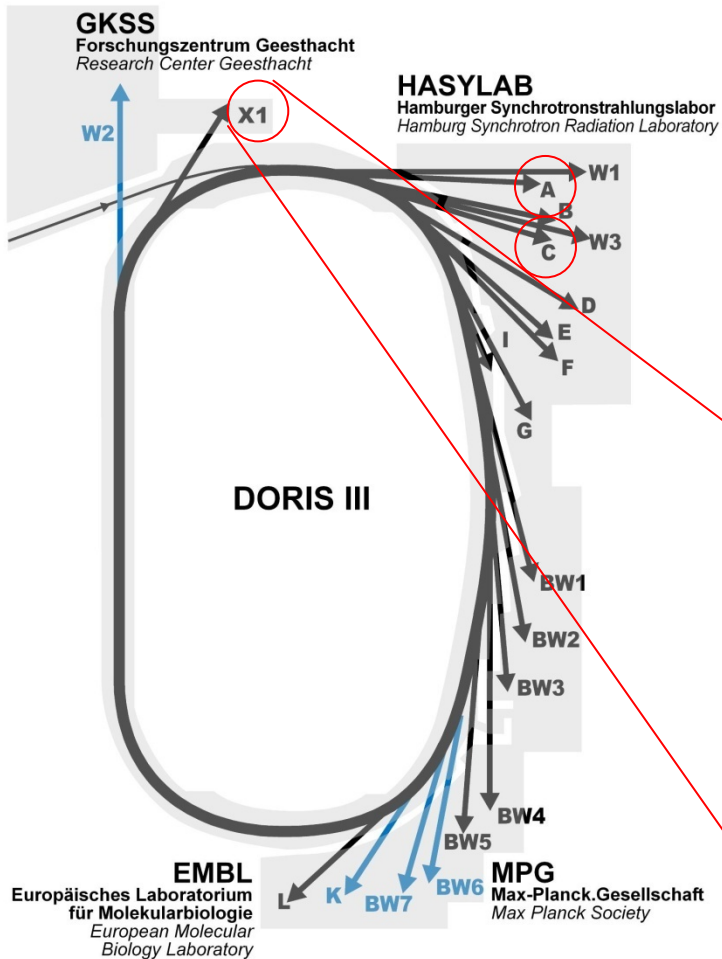 - plane polarization
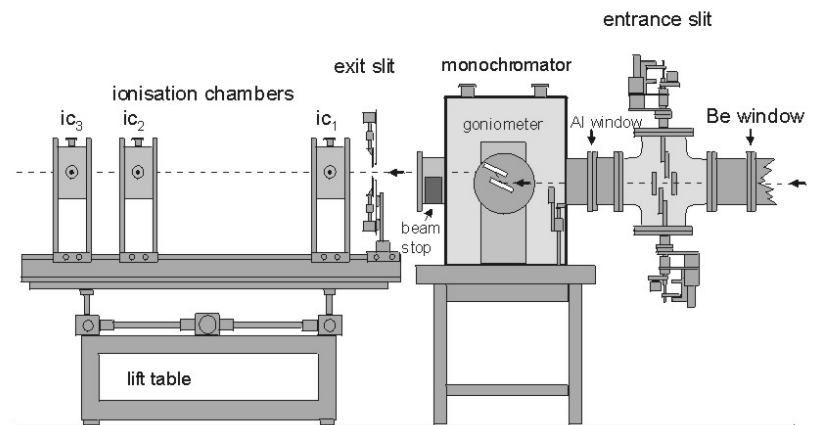 - time structure

Synchroton radiation

undulator beam

focussing magnets

electrons

wiggler

bending magnet

bending magnet beam

undulator

injection magnet

wiggler beam

acceleration section

wiggler

undulator

W. Bensch

Synchroton beamlines

synchroton beam

Undulator

e⁻

15 m
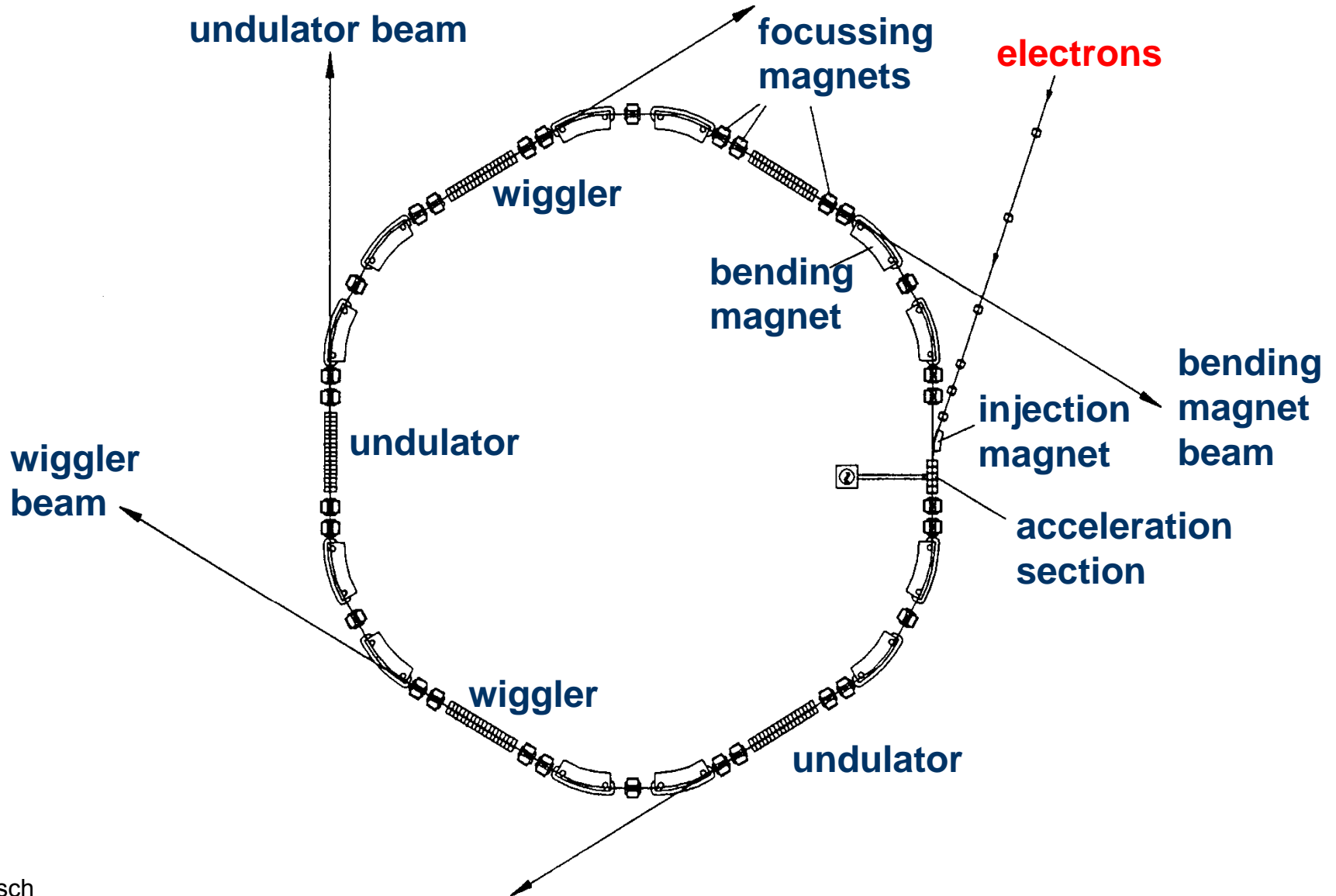
Undulator at HASYLAB, Hamburg

Brightness [Photons · s⁻¹ · mm⁻² · mrad⁻² · (0.1 % Bandwidth)⁻¹]

FELs

Undulators

Wigglers

Bending Magnets

X-Ray Tubes

Cu Kα rotating anode X-Ray tubes

T. Tschentscher

EXAFS at HASYLAB

Setup of the X1 experiment

Monochromators

Synchrotron

X-rays

Slit

Double Crystal Monochromator

Slit

Gas Feed

Ion Chamber

Catalytic Reaction Cell

Gas Chromatog
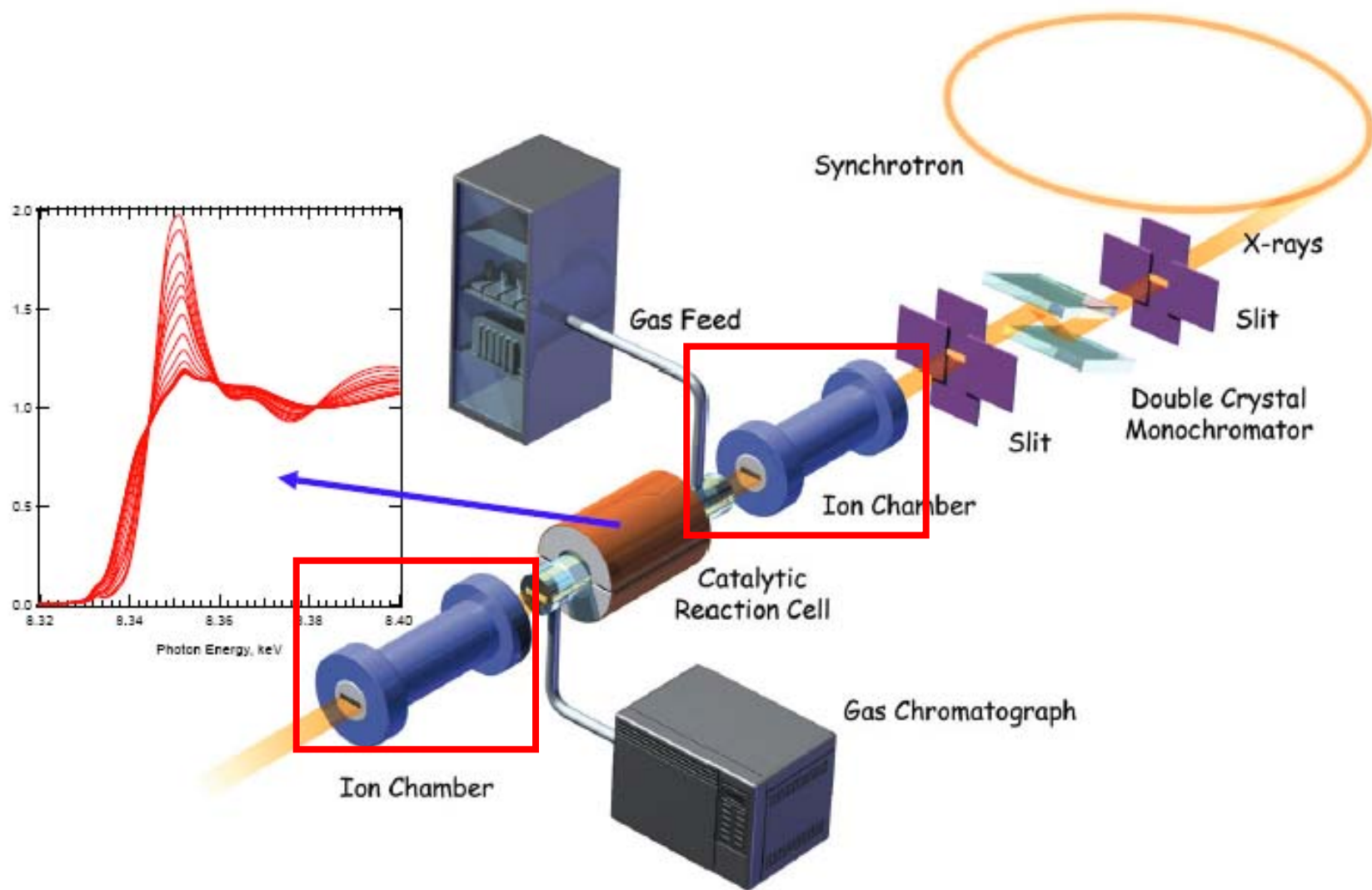
Ion Chamber

Photon Energy, keV
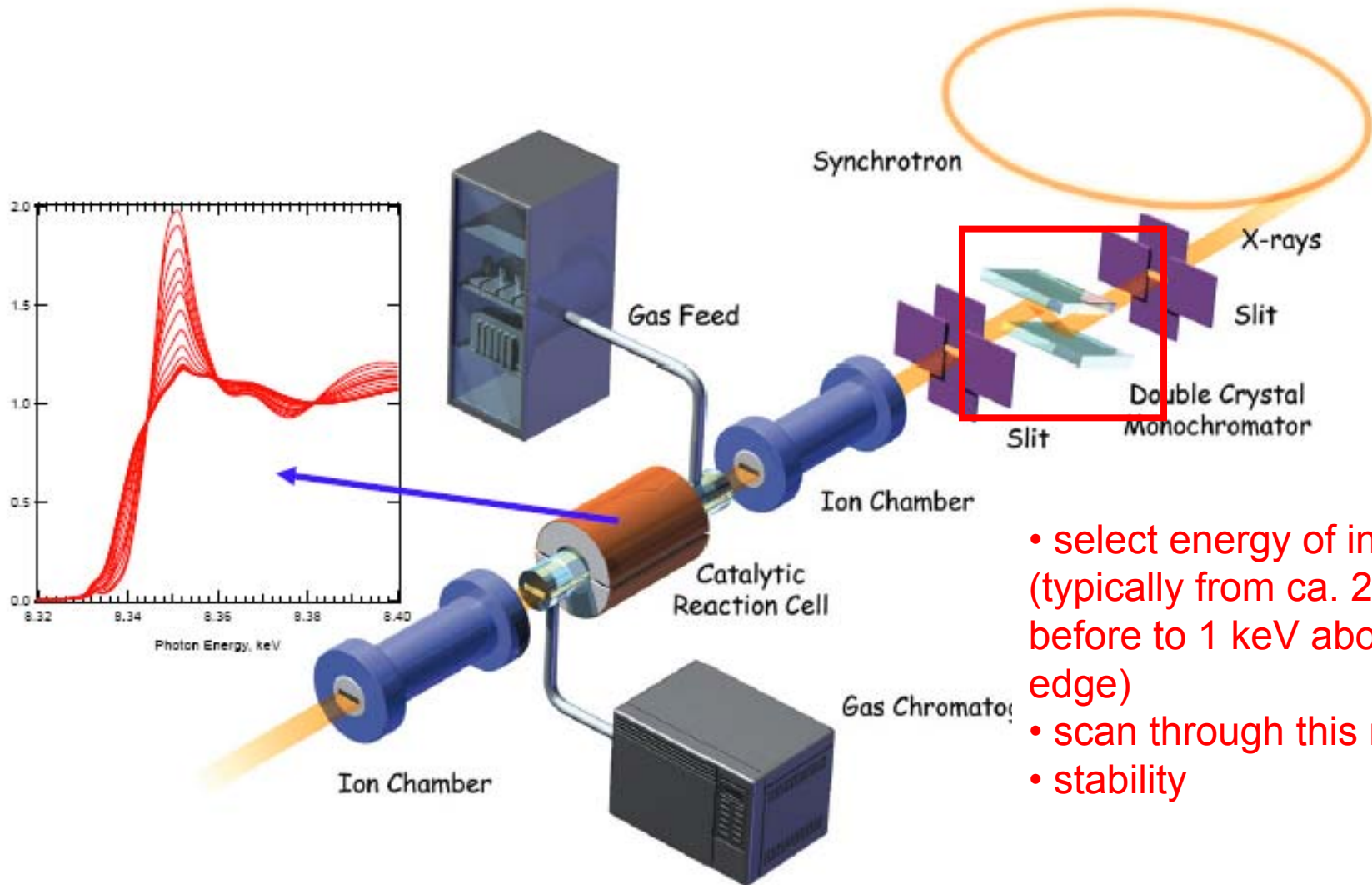
- select energy of interest (typically from ca. 200eV before to 1 keV above the edge)
- scan through this regime
- stability

Double single crystal monochromator
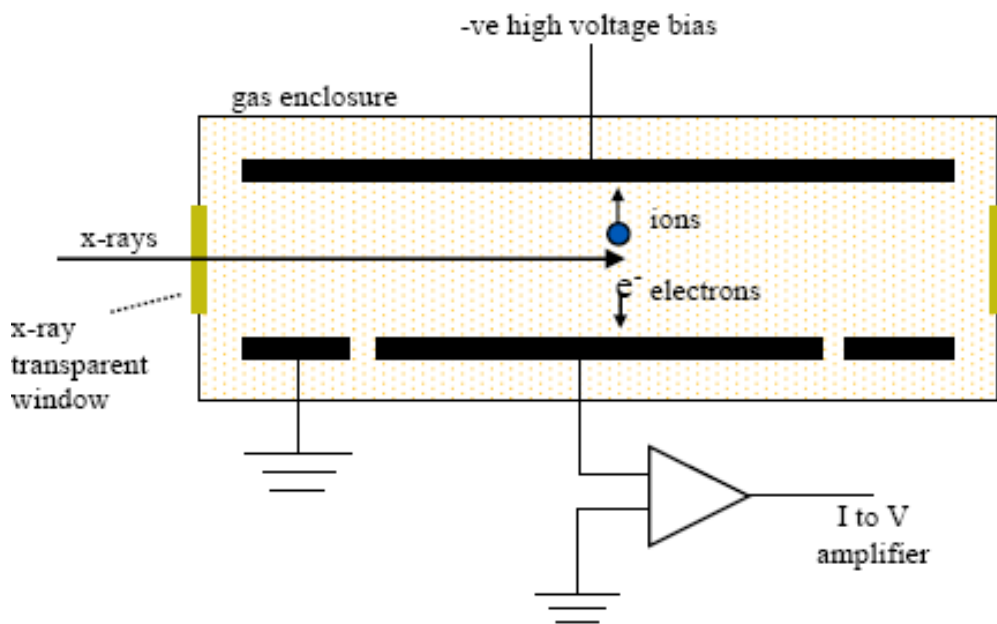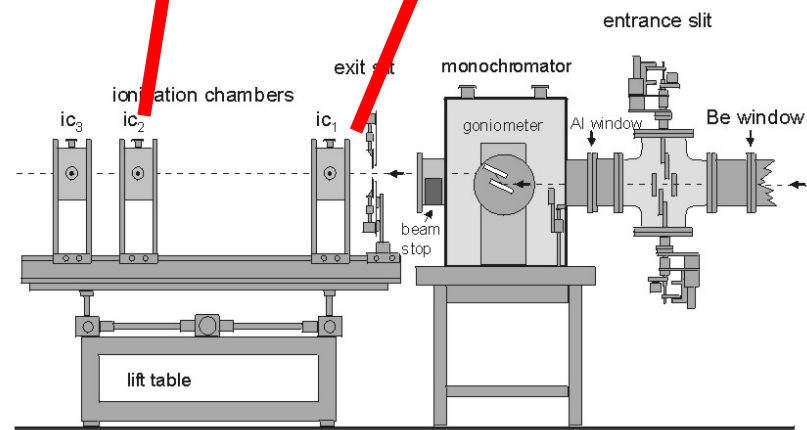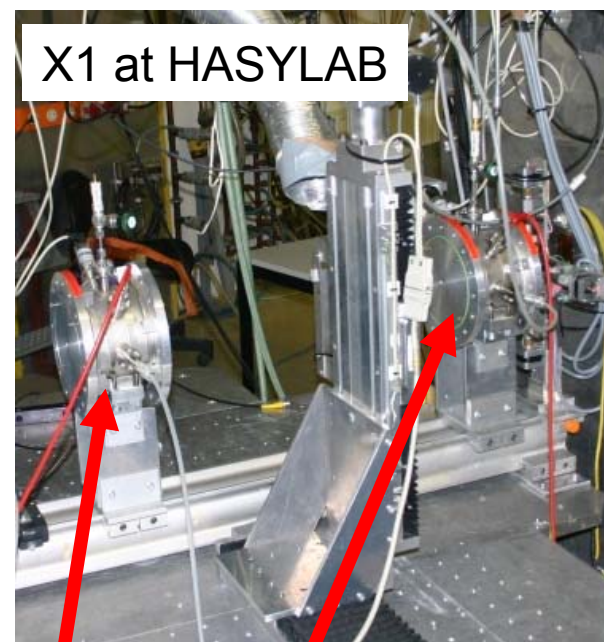
Si(111) crystal

monochromized
X-ray beam

Energy scanning by rotating θ

"white" X-ray beam

θ

X1 at HASYLAB

Available crystals:
Si 111: Energy range 7 - 20 keV
Si 311: Energy range 9 - 40 keV
Si 511: Energy range 11 - 100 KeV

α θ

d

θ

δ

$n \lambda = 2\, d_{hkl}\, \sin(\theta)$
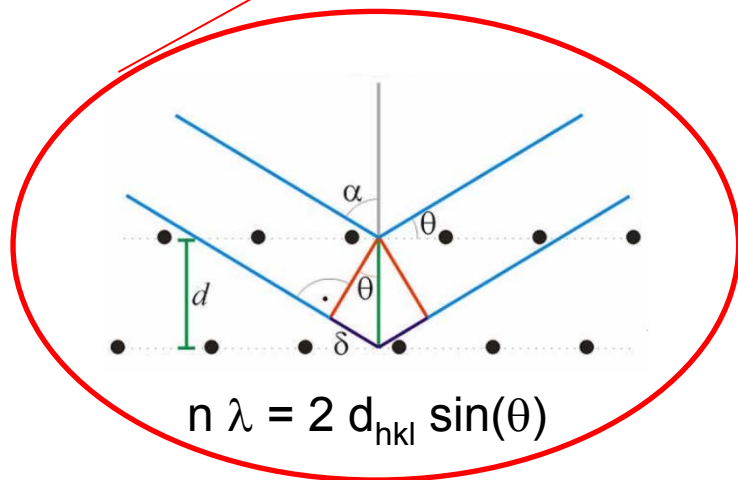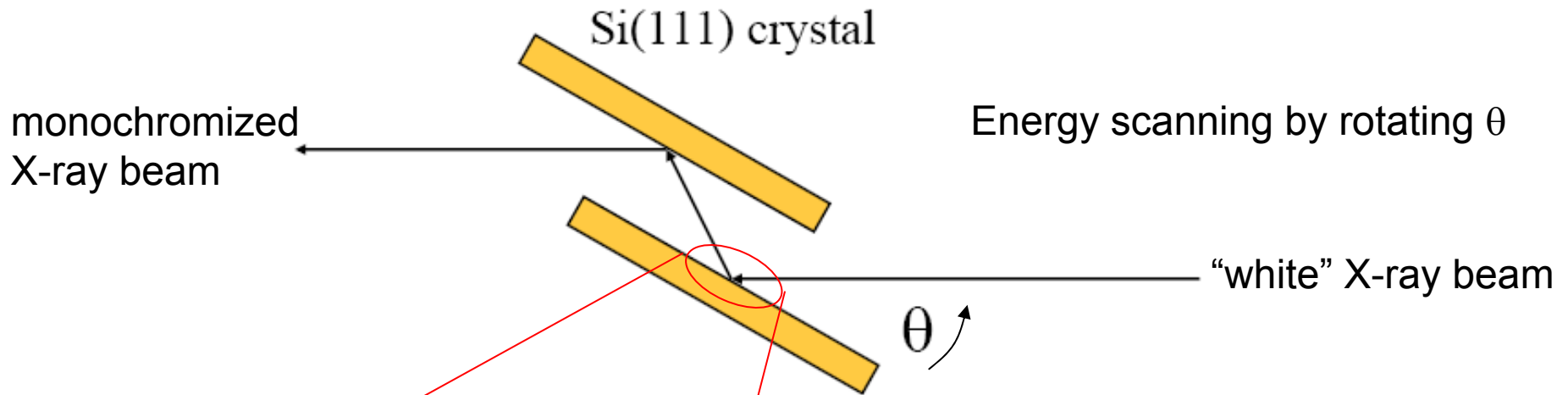
Detection: Transmission geometry

Ionization chambers

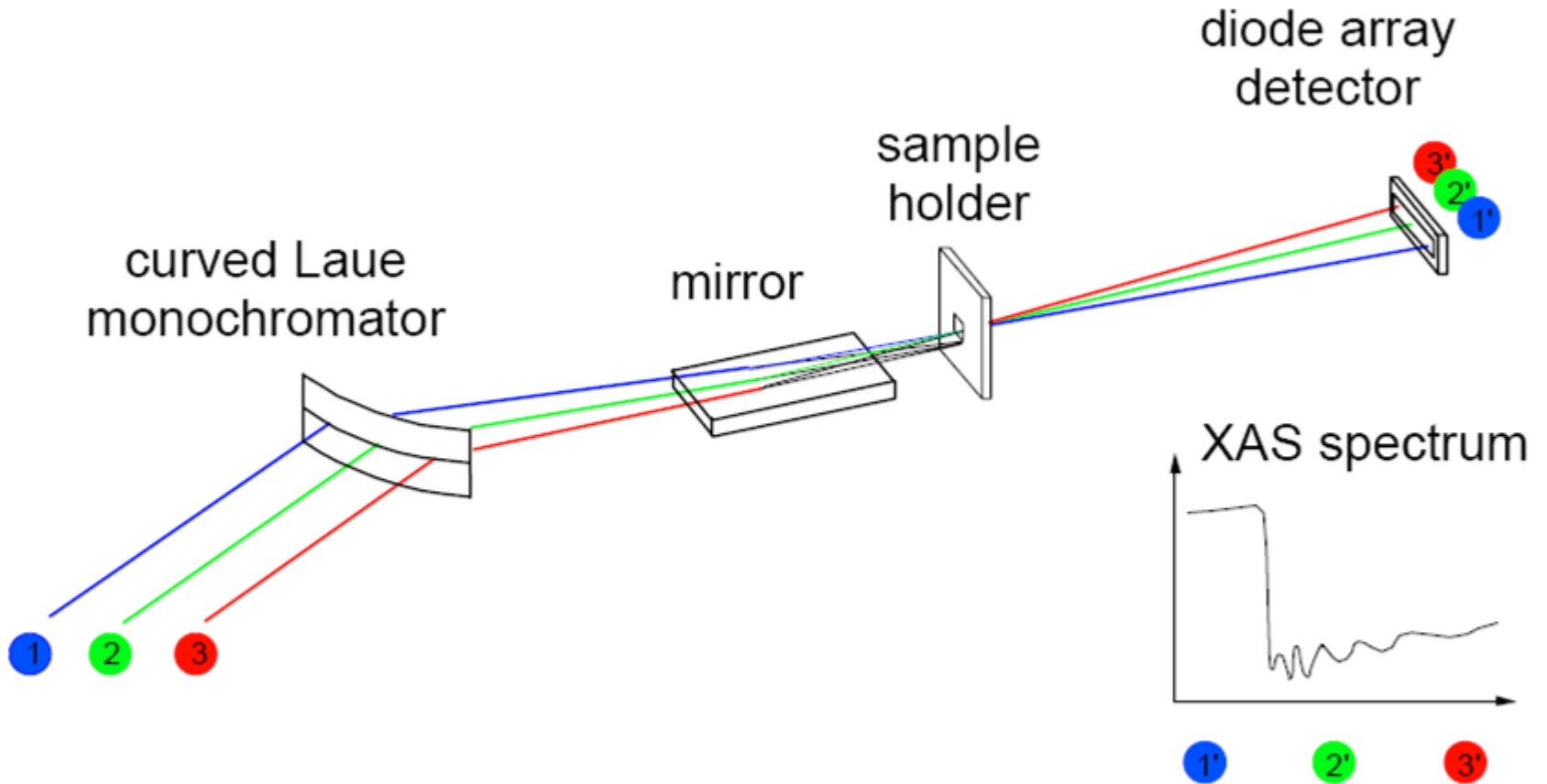X1 at HASYLAB

- Photon is absorbed by gas atom (He, N_2, Ar)
- Photoelectrons emitted (ionization)
- These electron initiate more ionization
- High voltage bias across plates causes electron and ions to drift in opposite directions.
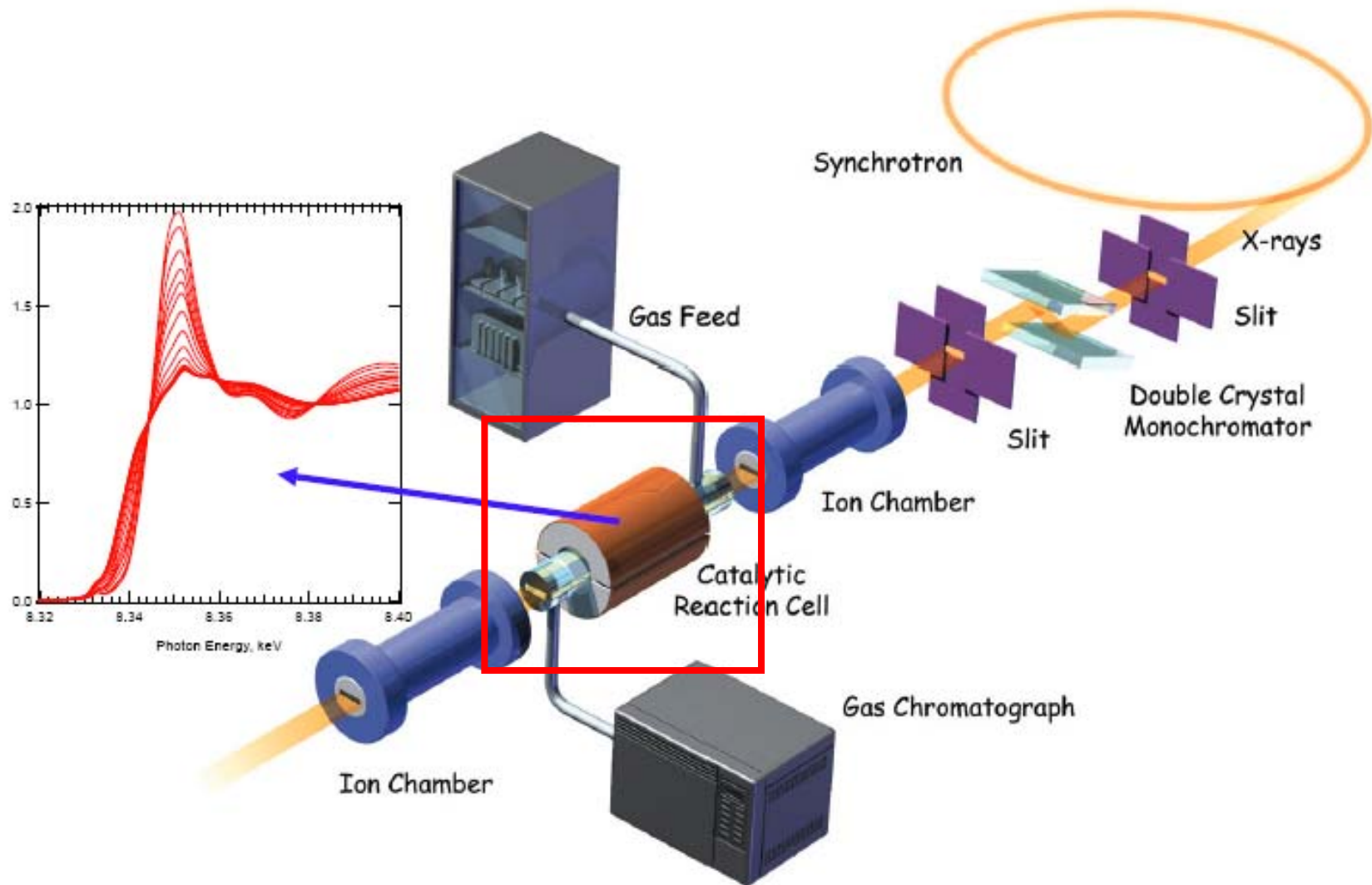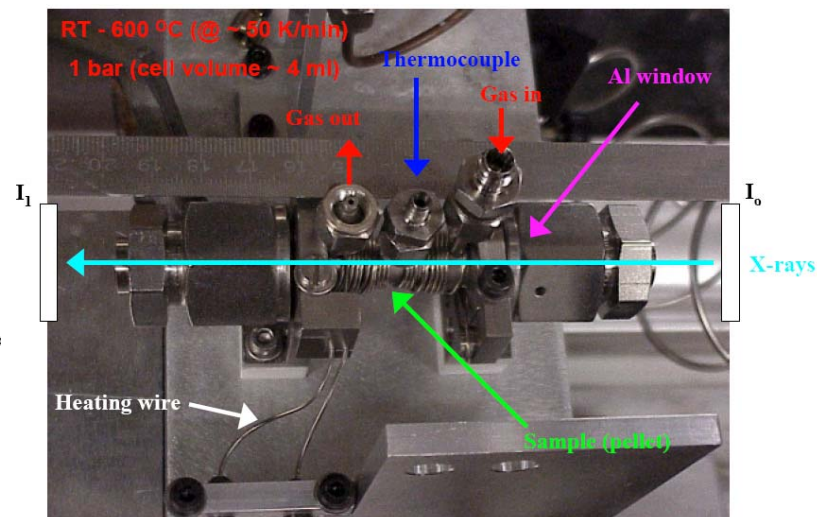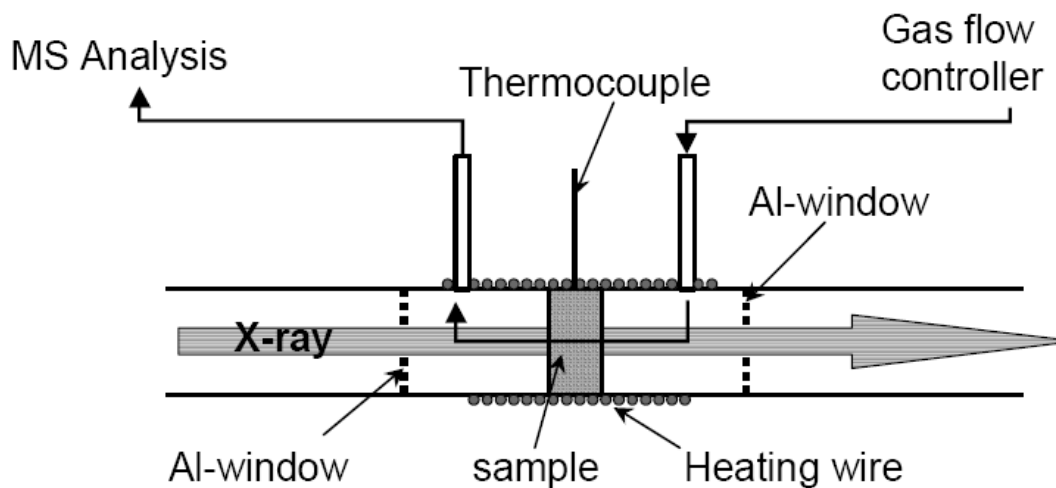- Charges collected result in current flow which is proportional to the incident x-ray intensity
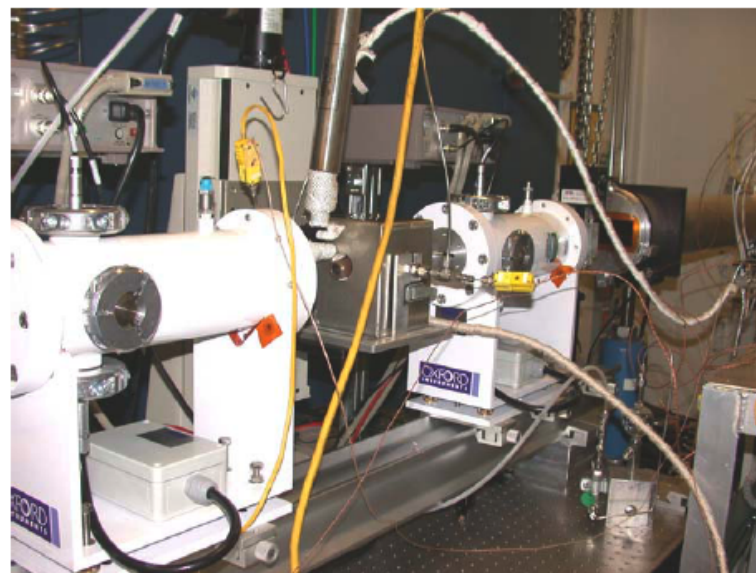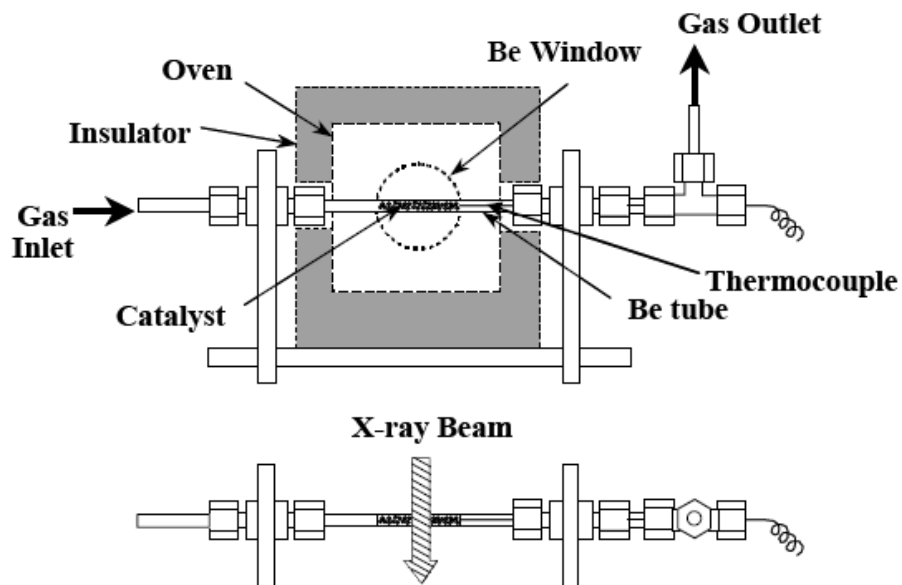
S. Bare

DXAFS

Energy-dispersive XAS (DXAFS), (ESRF, ID24), ~ s/spec

T. Ressler

Sample environment

Synchrotron

X-rays

Slit

Double Crystal
Monochromator

Slit

Gas Feed

Ion Chamber

Catalytic
Reaction Cell

Ion Chamber

Gas Chromatograph

Photon Energy, keV

S. Bare

Catalytic in-situ cells

MS Analysis

Thermocouple

Gas flow controller

Al-window

X-ray

Al-window   sample   Heating wire

T. Ressler

RT - 600 °C (@ ~ 50 K/min)
1 bar (cell volume ~ 4 ml)

Thermocouple

Gas out   Gas in   Al window

I_1 I_o

X-rays

Heating wire   Sample (pellet)

Gas Outlet

Be Window

Oven

Insulator

Gas Inlet

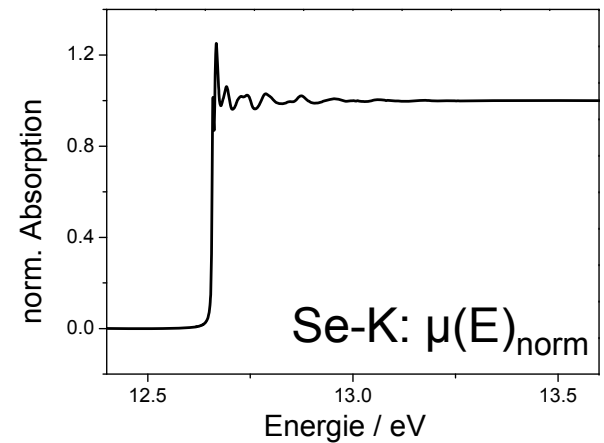Catalyst   Be tube
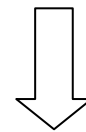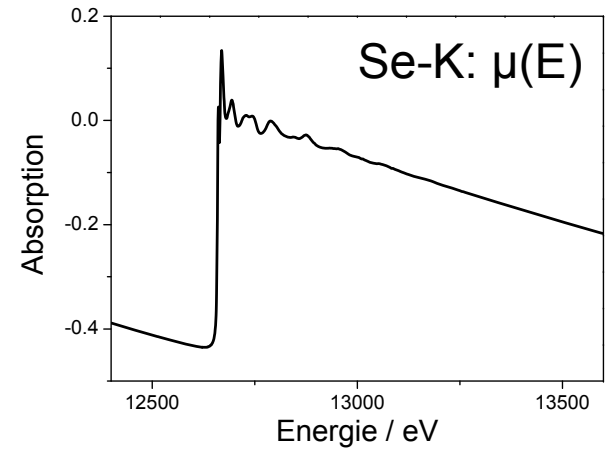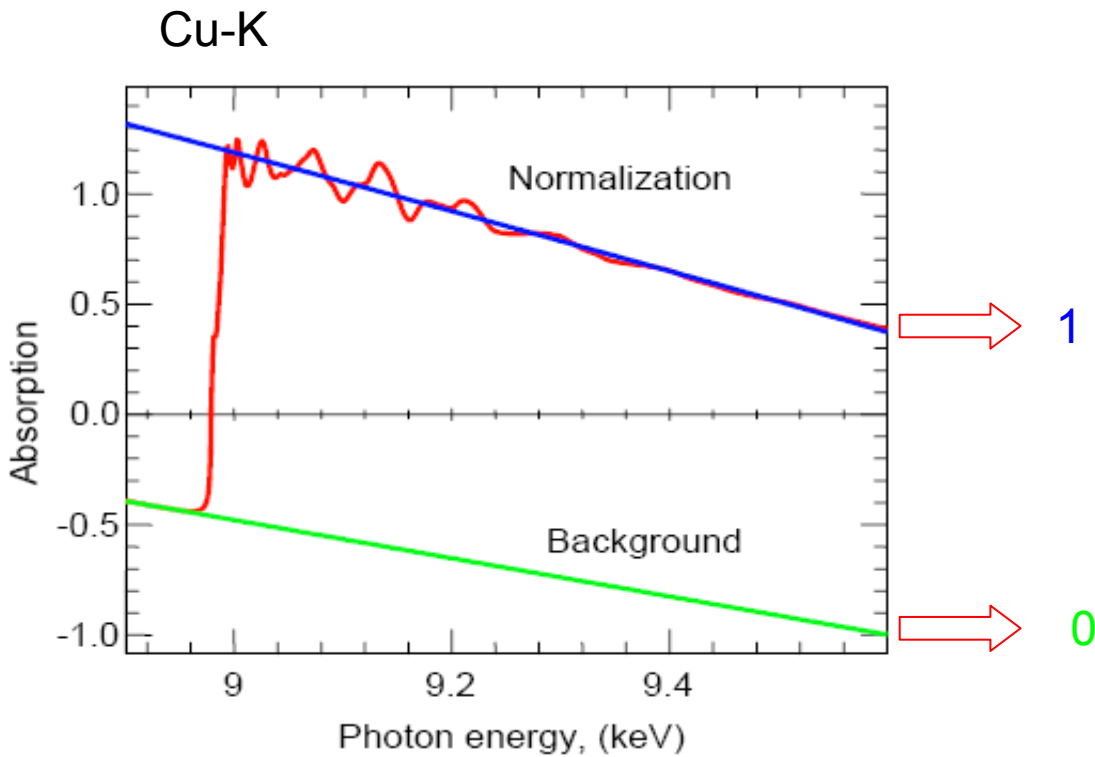
Thermocouple

X-ray Beam

S. Bare

Raw data treatment

- The spectrum μ(E) contains the EXAFS oscillations $\chi(E)$, which contain the structural information we are interested in.

- How to extract this information from the spectrum?

Subtraction of the "bare atom" background μ_0(E)

Division by the "edge step" $\Delta\mu_0$(E)

S. Bare
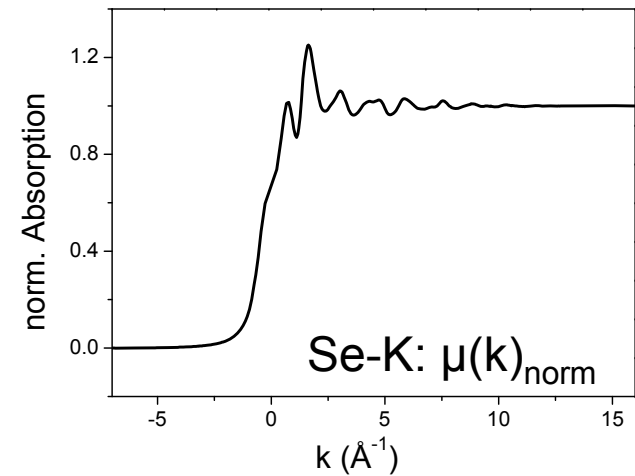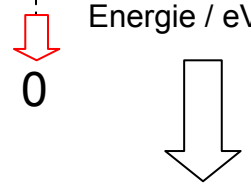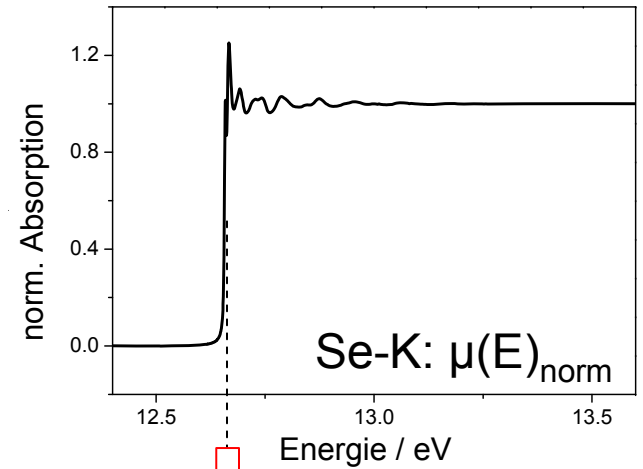
Normalization

T. Ressler
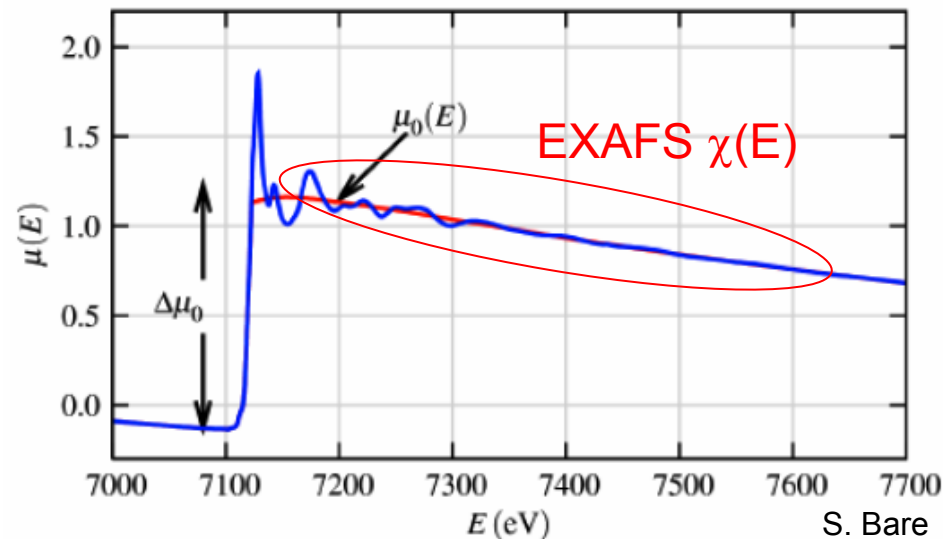
Transformation μ(E)$_{norm}$ → μ(k)$_{norm}$

EXAFS is an interference effect that depends on the wave nature of the photoelectron. It is therefore convenient to think of EXAFS in terms of the photoelectron wavenumber, *k*, rather than x-ray energy

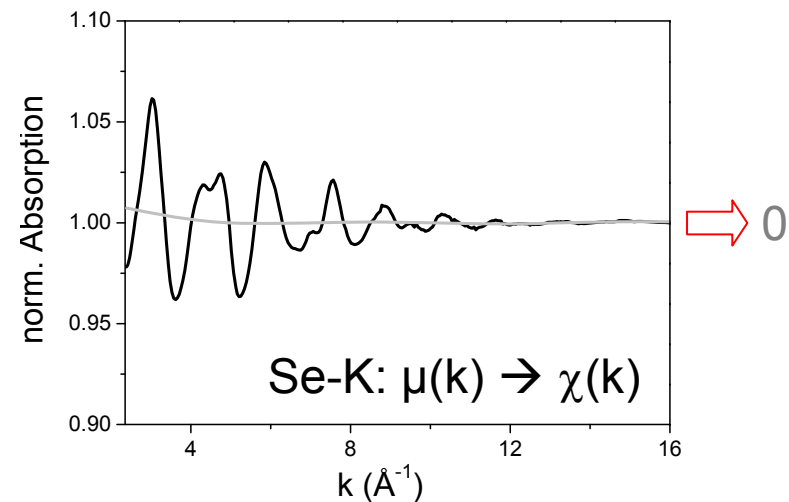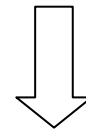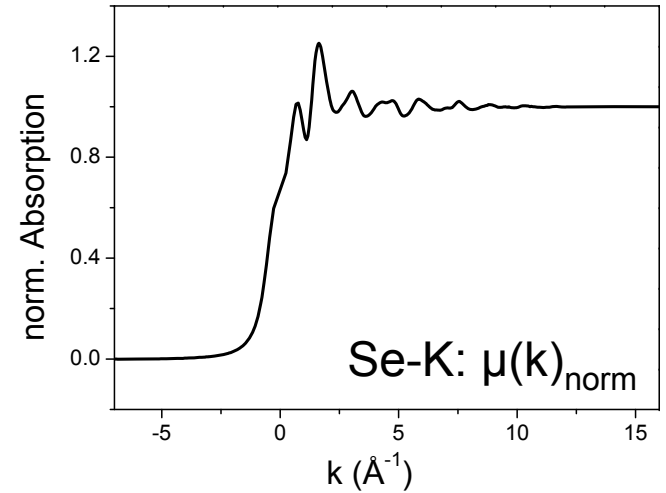$$k = \sqrt{\frac{8\pi^2 m_e}{h}(E - E_0)}$$

m$_e$:   mass of electron
E: Energy of incoming photon
E$_0$:   Threshold energy at absorption edge

Se-K: μ(E)$_{norm}$

0

Se-K: μ(k)$_{norm}$

$\mu_0(k)$ Fit

EXAFS oscillations are extracted from $\mu(k)_{norm}$ by subtraction of the "bare atom" background $\mu_0(k)$ and normalizing

$$\chi(k) = \frac{\mu(k) - \mu_0(k)}{\mu_0(k)}$$

Se-K: $\mu(k)_{norm}$
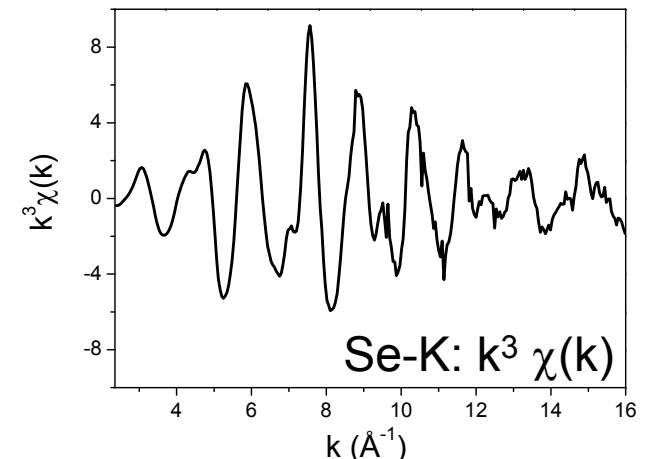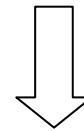

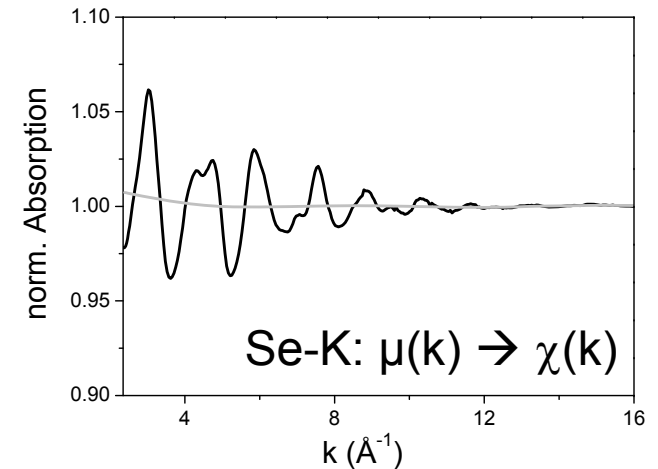Se-K: $\mu(k) \rightarrow \chi(k)$

k-Weighting

χ(k) is typically weighted be k^2 or k^3 to amplify the oscillations at high k.

One way to separate the sine waves (scattering paths) from one another is to perform a Fourier transform.

For the Fourier transformation it is best when the amplitudes of c(k) are similar thourght χ(k)

Se-K: μ(k) → χ(k)

Se-K: k^3 χ(k)

Fourier transformation

The resulting magnitude of the transform now has peaks representative of the different scattering paths of the photoelectron

→ Radial distribution function FT(χ(k))

Se-K: $k^3 \chi(k)$

cugr0l_cxe

Se-K: FT($k^3\chi(k)$)

S. Bare
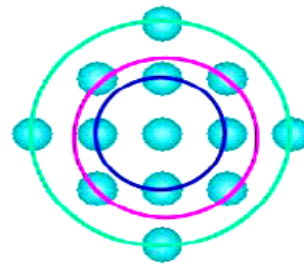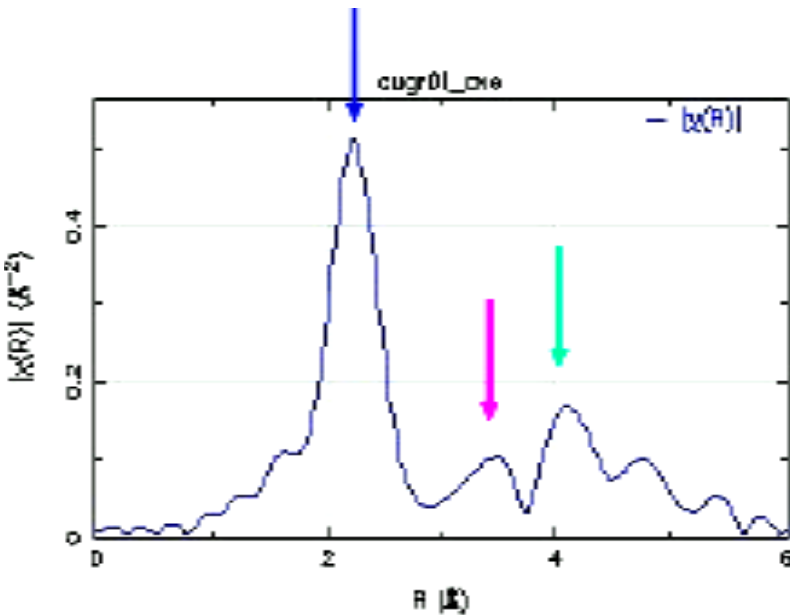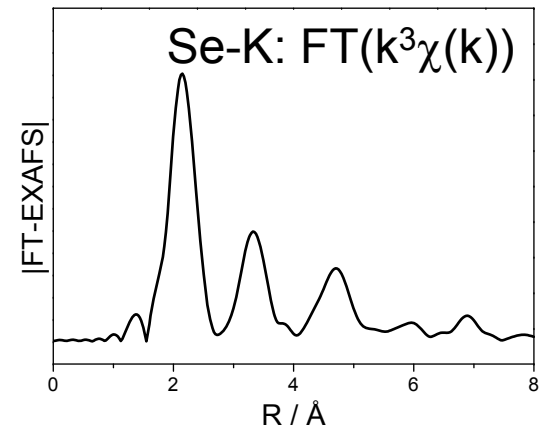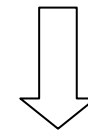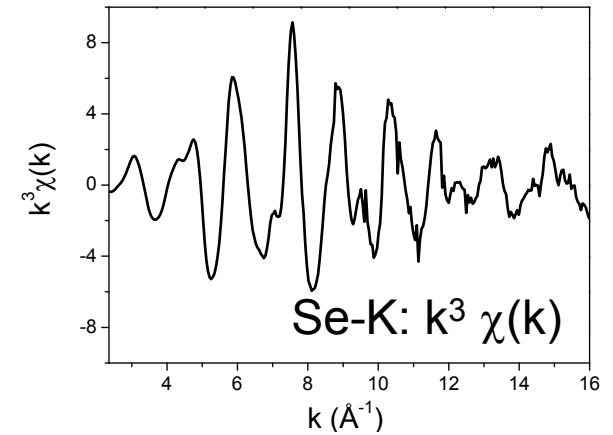
Scattering paths

Mo Metal (bcc)

FT →

1st shell

2nd shell

R_1 R_2^R [Å]

R2

R1

1st shell
(2.73 Å)

2nd shell
(3.14 Å)

T. Ressler

The EXAFS equation

$$\chi(k) = S_0^2 \sum_i N_i \frac{\left|f_i(k)\right|}{kR_i^2} e^{(-2\sigma_i^2 k^2)} e^{(-2R_i/\lambda(k))} \sin(2kR_i + 2\delta_i + \varphi_i)$$

N_i — is the number of scattering atoms of type i

R_i — is the distance from the central atom to the scattering atom
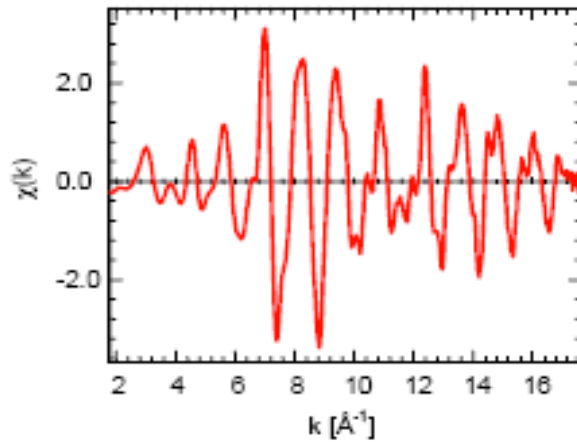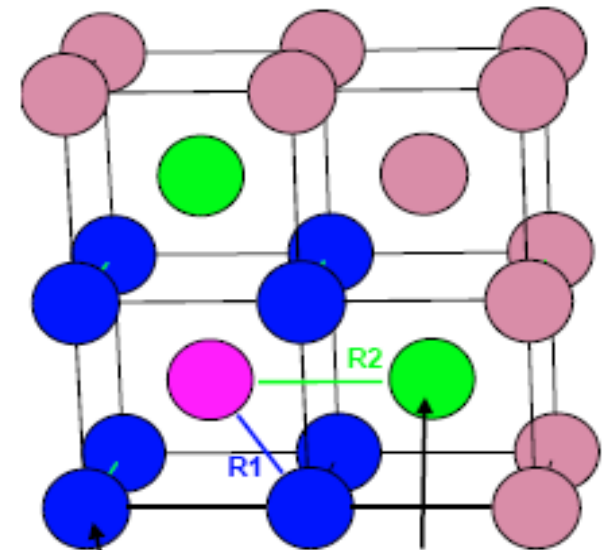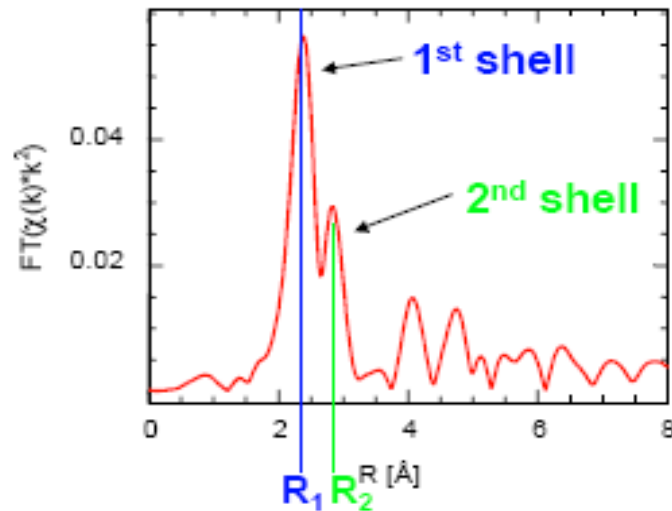
S_0^2 — is the amplitude reduction factor (due to multielectron processes).

$e^{(-2\sigma_i^2 k^2)}$ — is a term to account for the disorder in the position of the atoms.

$e^{(-2R_i/\lambda(k))}$ — is a damping factor to account for the fact that the photoelectron wave is only scattered elastically over a short distance.

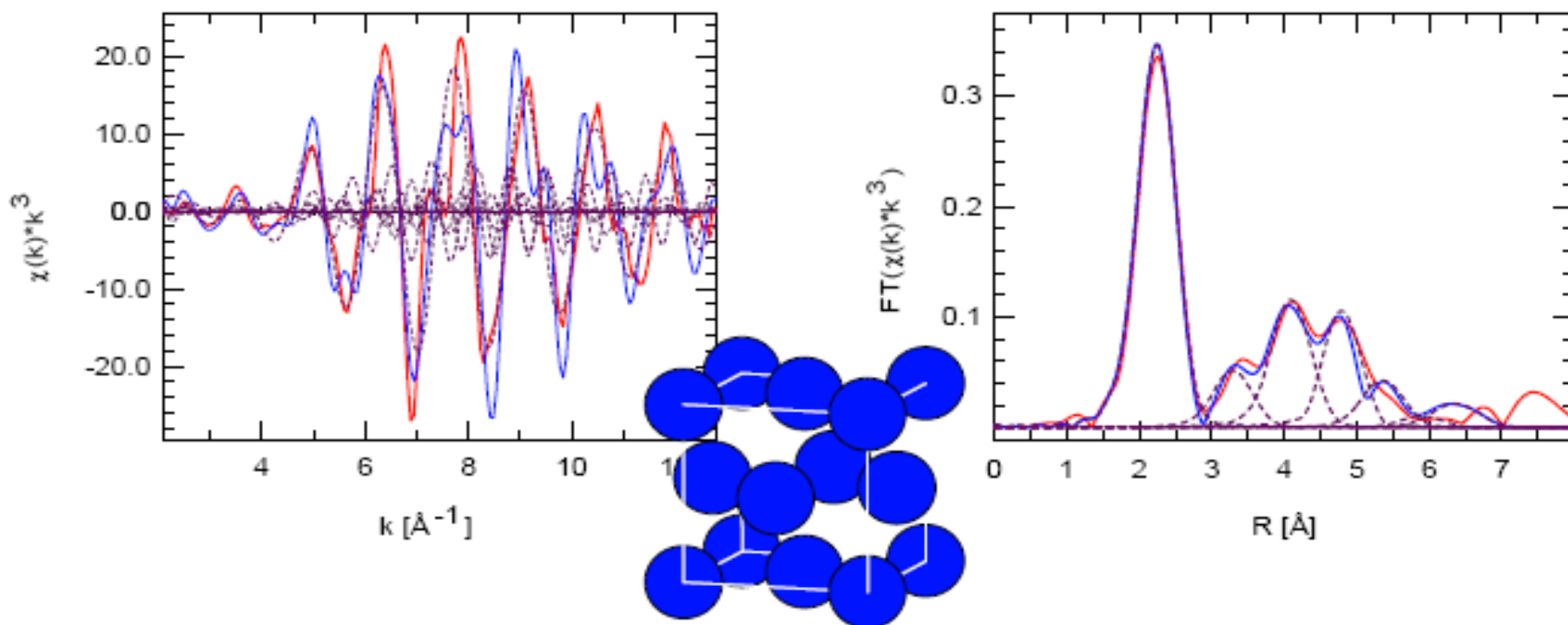$f_i(k)$ — is the scattering amplitude at atom i

δ_i — is the phase shift undergone by the photoelectron at the central atom

φ_i — is the phase shift undergone by the photoelectron when it bounces off the scattering atom

S. Bare

Fitting of EXAFS data

$$\chi(k) = \sum_j \frac{N_j S_0^2 F_j(k)}{kR_j^2} \cdot e^{\left(-2k^2\sigma_j^2\right)} \cdot e^{\left(\frac{-2R_j}{\lambda}\right)} \cdot e^{\left(\frac{2}{3}\sigma_j^{(4)}\right)} \cdot \sin\left[2kR_j + \delta_j(k) - \frac{4}{3}\sigma_j' k^3\right]$$

Structural model: backscattering amplitudes and phase shifts from reference spectra or calculated *ab initio* (e.g. FEFF code) and starting parameters

Fitted parameters: Least squares fitting (e.g. WinXAS package)

EXAFS Fitting: Cu LDH
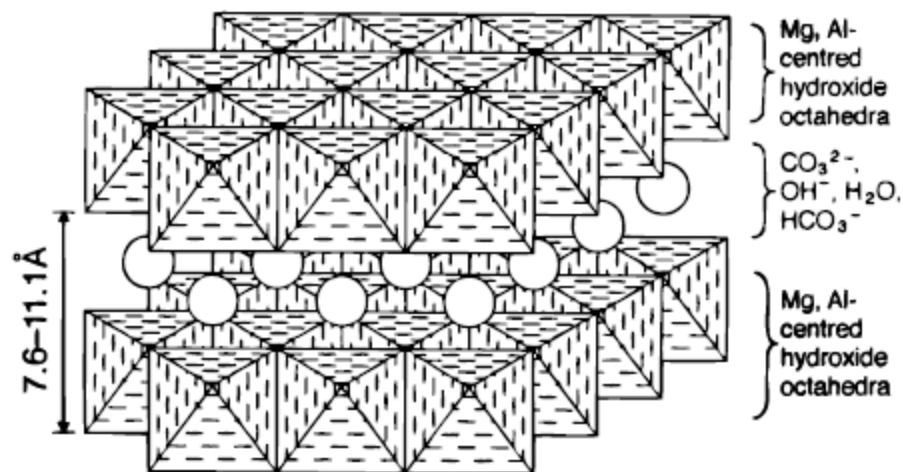
Layered double hydroxide:

$(Mg,Cu)_{1-x}(OH)_2Al_x(CO3)_{2/x} \cdot m\ H_2O$

10 % Cu: Is it in or between the layers?

Cu-K EXAFS fitting

contribution	functions j		N_j	$R_j/\text{Å}$	$\sigma_j^2/\text{Å}^2$	$\Delta E_0/\text{eV}$	R
Cu—O	1st	O	4.8	1.99	0.006	5.4	0.11
(two-shell fit)	2nd	O	1.6	2.25	0.003		
Cu⋯Al		Al	4.3	3.05	0.006	6.0	0.22
(one-shell fit)							
Cu⋯Mg		Mg	4.3	3.07	0.006	3.5	0.26
(one-shell fit)							
Cu—O+	1st	O	4.6	1.98	0.005	5.3	
Cu⋯Al/Mg	2nd	O	2.8	2.24	0.009	5.3	0.10
(three-shell fit)	3rd	Al	4.6	3.05	0.007	4.0	

[a] In all curve-fitting procedures the amplitude reduction factor was kept fixed at $S_0^2 = 0.85$. [b] Estimated error of the distances: 0.03 Å.

⇒ Cu^{2+} is incorporated in the LDH layers

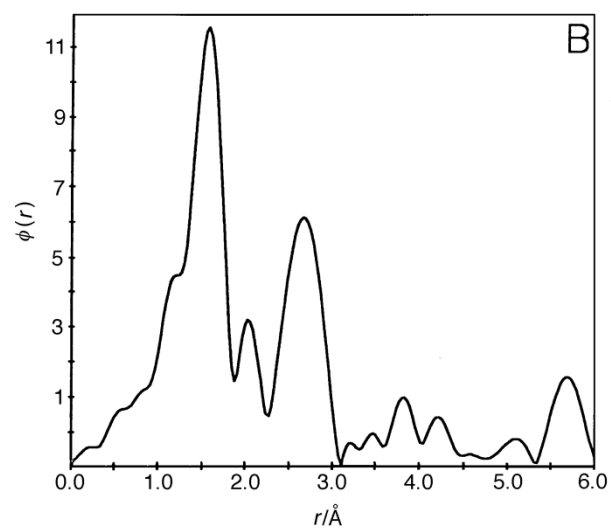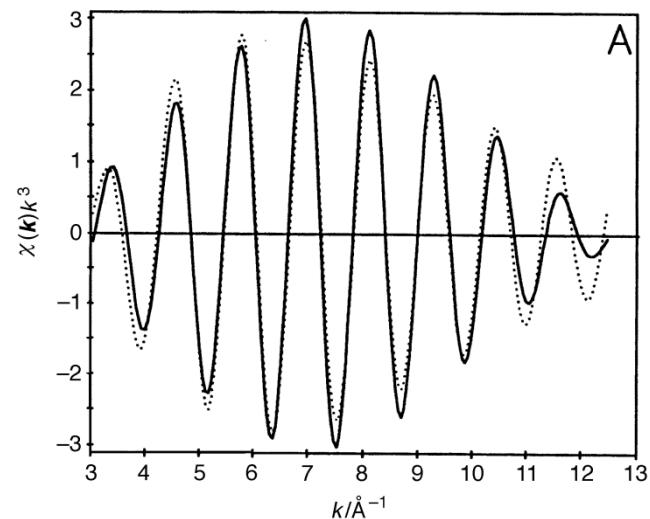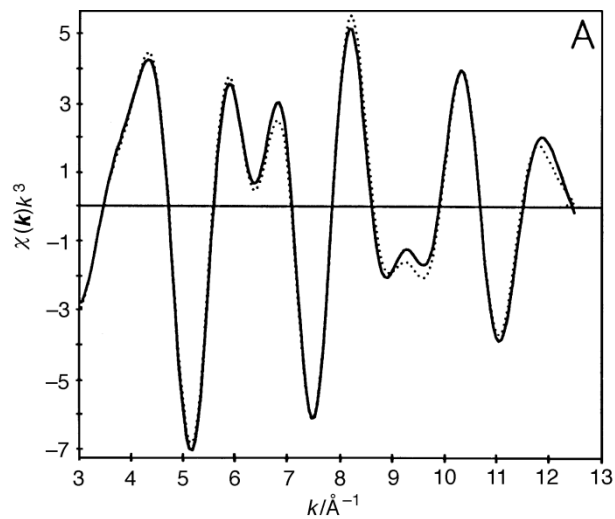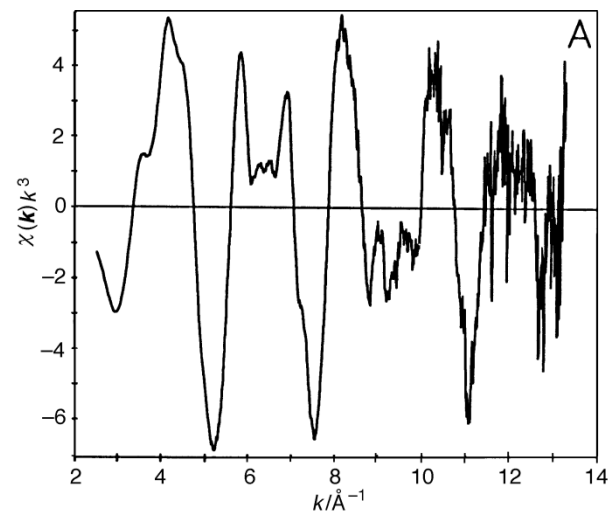Köckerling, Geismar, Henkel Nolting, J. Chem. Soc., Faraday Trans., 1997, 93(3), 481.

Cu LDH: Spectra
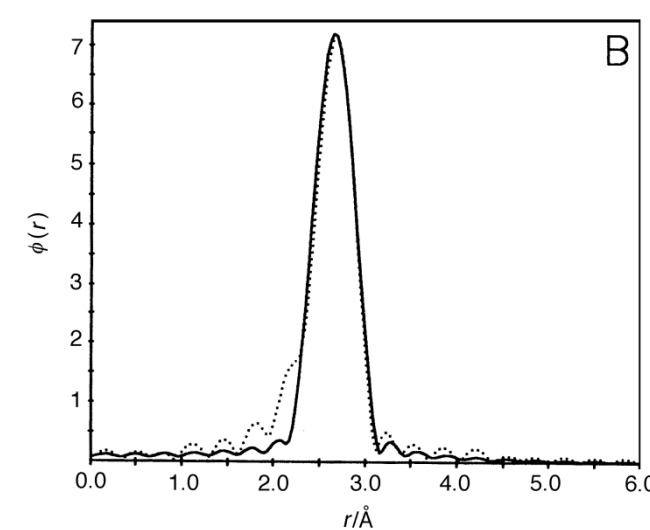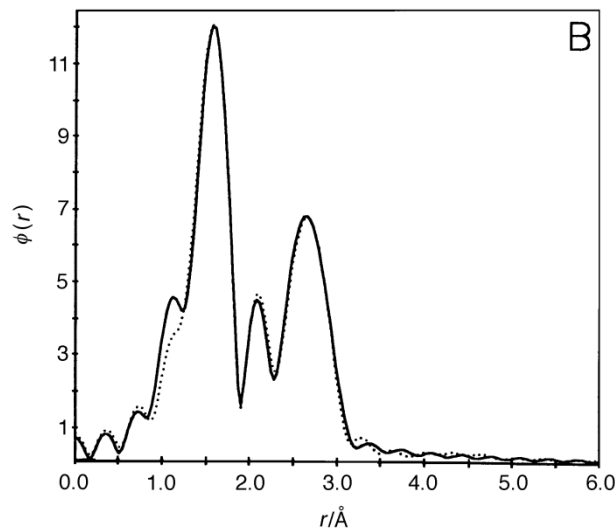
Experimental　　　　　　　　　Fourier filtered: first three shells　　Fourier filtered: third shell

EXAFS fitting: metal ordering in aurichalite

Problem: Cu/Zn ordering in aurichalcite (a possible precursor for Cu/ZnO catalysts)

Aurichalcite: $(Cu,Zn)_5(CO_3)_2(OH)_6$

XRD crystal structure:

P 2_1/m, monoclinic

a=13.8200 Å; b=6.4190 Å
c=5.2900 Å; β=101.04°
(40% Cu)

No distinction of Cu and Zn possible with XRD

Harding, M.M.;Kariuki,
B.M.;Cernik, R.;Cressey, G.,
Acta Cryst. B **50,** 1994, 673.

2 M1

2,24
2,13
1,94
2,03
2,24
2,13
M1

4 M2

2,31
2,01
2,01
2,00
1,93
2,38

2 M3

1,97
1,95
1,95
2,00
1,95

2 M4

2,02
1,98
2,36
2,14
1,98
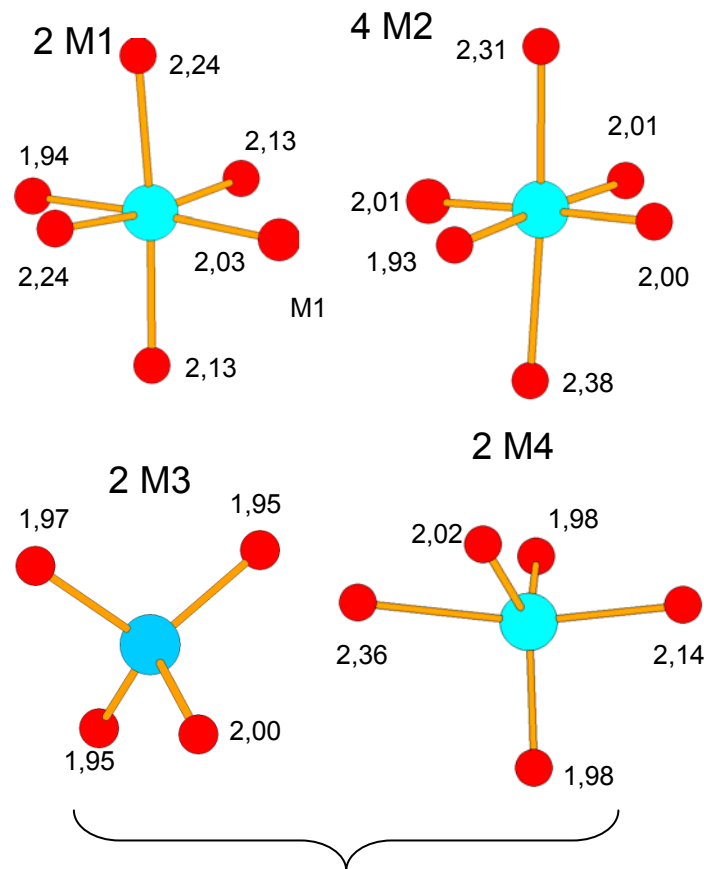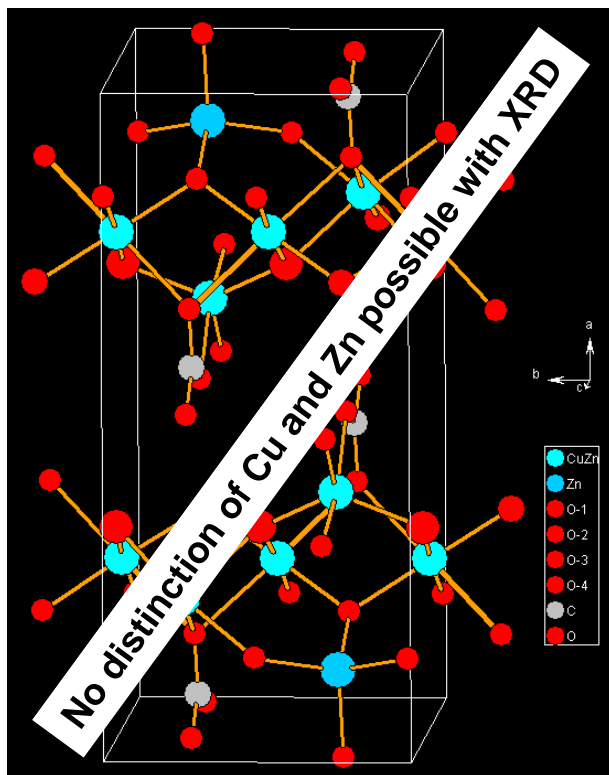
Structural model: Starting parameters for EXAFS fit

Cu/Zn ordering

Cu-K EXAFS

FIG. 4. (a) 80K Cu EXAFS (solid lines) and the corresponding best fits (broken lines) of aurichalcite. BM 1964,702 (top), BM 1983,97 (middle) and BM 1937,1355 (bottom). (b) Fourier transforms of the 80K Cu EXAFS (solid lines) and the corresponding best fits (broken lines) of aurichalcite. BM 1964,702 (top), BM 1983,97 (middle) and BM 1937,1355 (bottom).
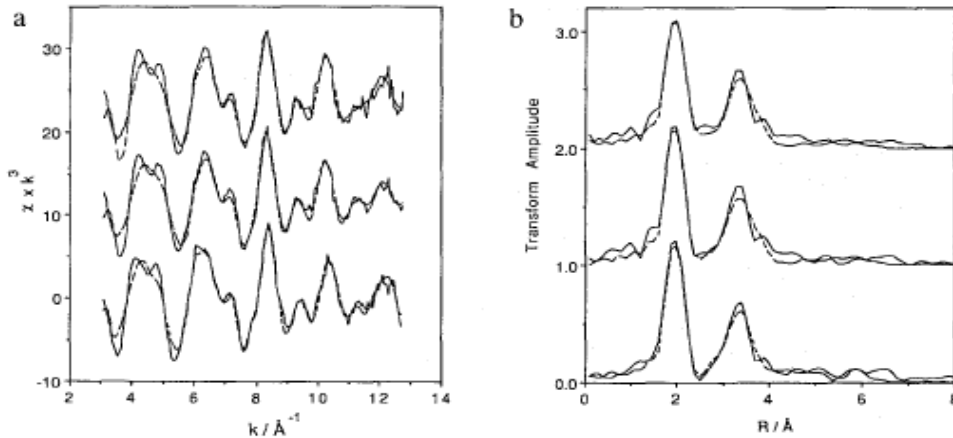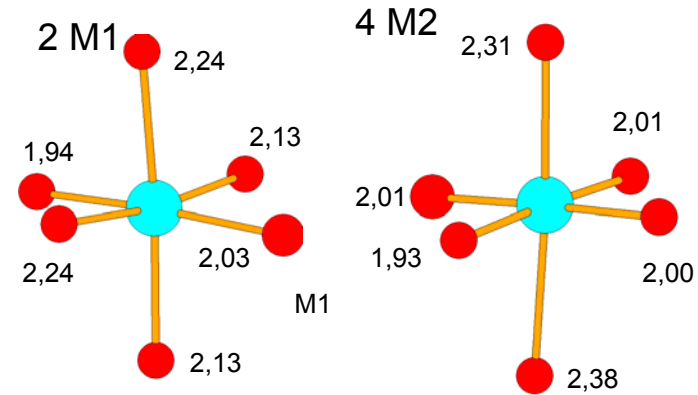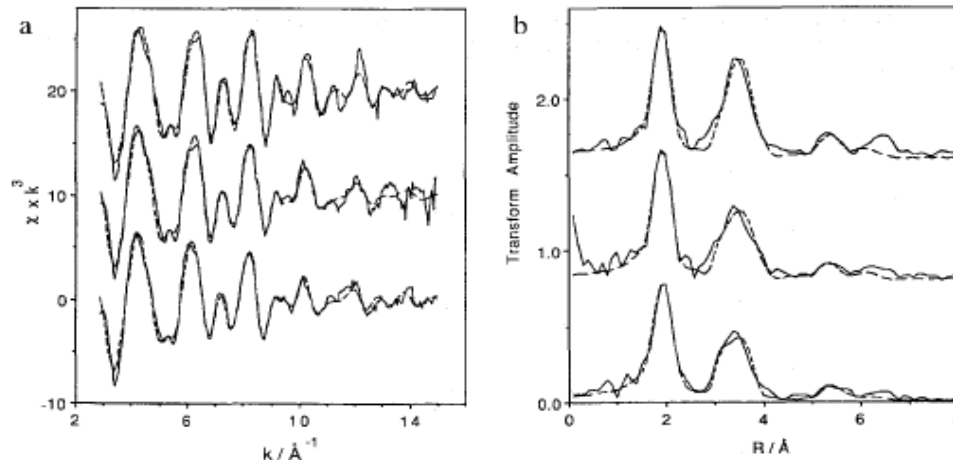
Zn-K EXAFS

FIG. 5. (a) 80K Zn EXAFS (solid lines) and the corresponding best fits (broken lines) of aurichalcite. BM 1964,702 (top), BM 1983,97 (middle) and BM 1937,1355 (bottom). (b) Fourier transforms of the 80K Zn EXAFS (solid lines) and the corresponding best fits (broken lines) of aurichalcite. BM 1964,702 (top), BM 1983,97 (middle) and BM 1937,1355 (bottom).

2 M1 2,24 1,94 2,13 2,24 2,03 2,13 M1
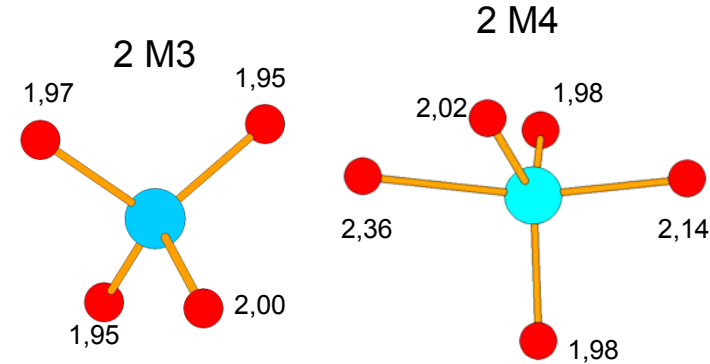
4 M2 2,31 2,01 2,01 1,93 2,00 2,38

Cu on M2 (80%) & M4
Zn on M1 & M3

2 M3 1,97 1,95 1,95 2,00

2 M4 2,02 1,98 2,36 2,14 1,98

J.M. Charnock, P.F. Schofield, C.M.B. Henderson, G. Cressey, B.A. Cressey, Mineral. Mag. 1996, 60, 887

EXAFS in catalysis
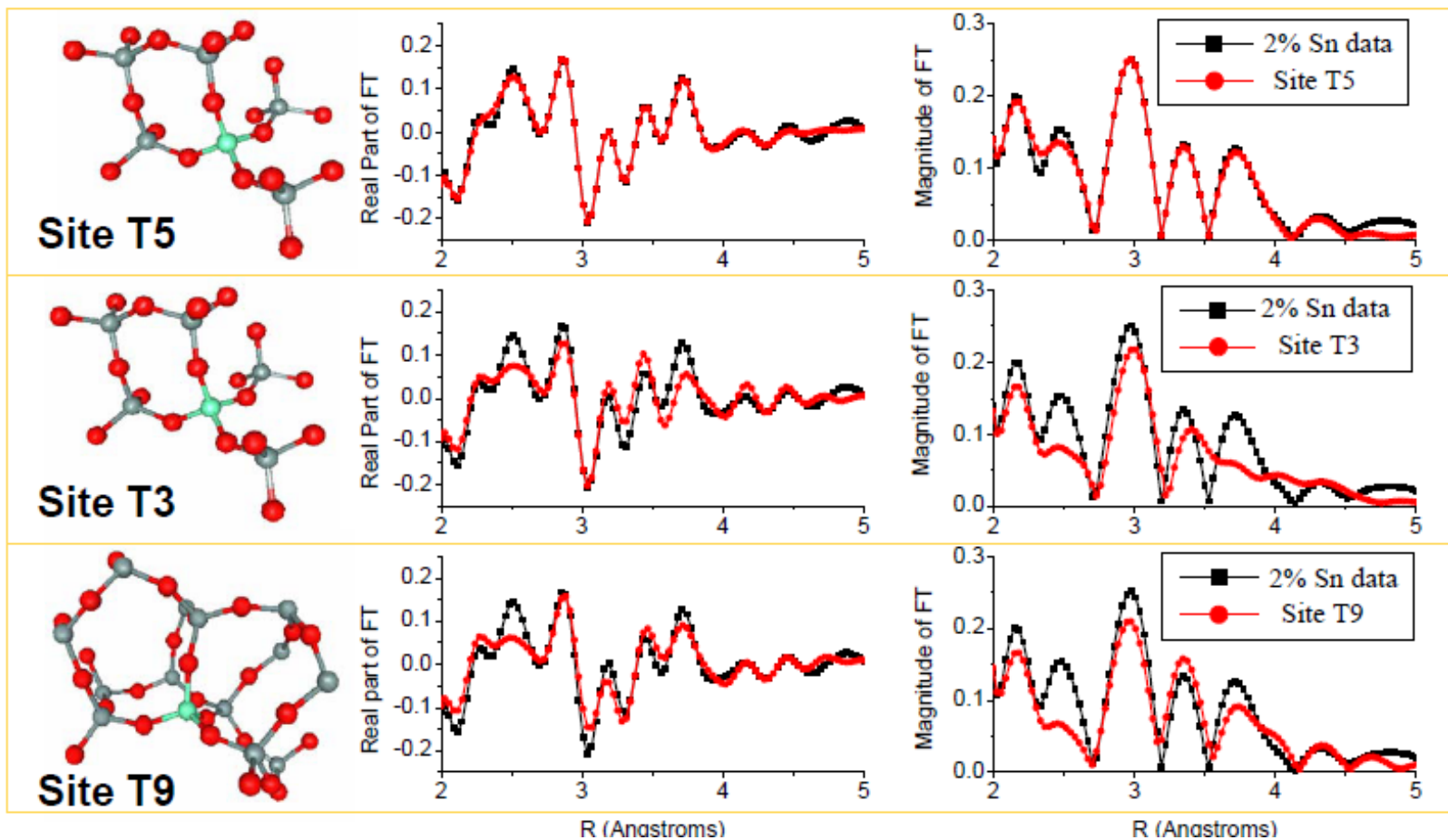
Sn resides on the T5 site of beta-zeolite !

S. Bare

In-situ XAFS

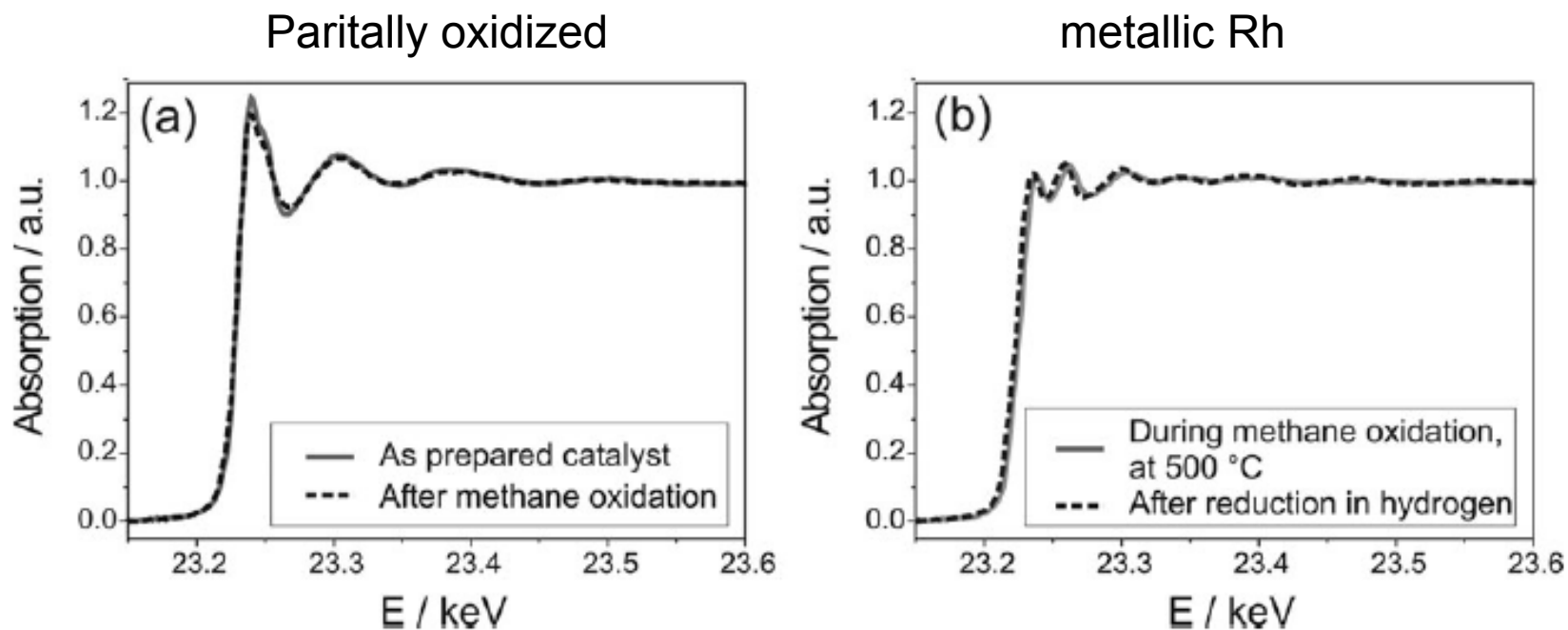Paritally oxidized   metallic Rh

Rh-Pt/Al_2O_3 catalyst in partial oxidation of methane

Grunwaldt, Baiker, Phys . Chem. Chem. Phys., 2005, 7, 3526.

EXAFS Summary

- EXAFS oscillations $\chi(k)$ are due to interference of the photoelectron wave coming from the absorber atom and backscattered waves from the neighboring atoms, various scattering paths contribute

- The shape of $\chi(k)$ is determined by the local environment around a specific element

- $\chi(k)$ contains information on the neighboring atom type, the inter-atomic distances and the coordination number

- A well develped theory is available to extract this information from experimental data by least-squares fitting (careful data reduction necessary)

- EXAFS works on all kinds of material, most elements and can be applied in-situ

- Synchroton radiation is required

Literature / references

- D.C. Koningsberger, R. Prins (ed.): "X-Ray Absorption" John Wiley & Sons, New York 1982

- D. Koningsberger, D. E. Ramaker: "Application of X-Ray Absorptions Spectroscopy in Heterogeneous Catalysis: EXAFS, Atomic XAFS and Delta XANES" in Handbook of Heterogeneous Catalyis (Ertl, Knözinger, Schüth, Weitkamp), Wiley

- Lecture scripts of Simon Bare (UOP), Thorsten Ressler (TU Berlin), Wolfgang Bensch (Uni Kiel)